九州大学学術情報リポジトリ
Kyushu University Institutional Repository

Spatio-temporal streamflow generation under changing environment in a small forested headwater catchment

孫, 昊田

https://doi.org/10.15017/1866351

出版情報：九州大学, 2017, 博士（農学）, 課程博士
バージョン：
権利関係：

Spatio-temporal streamflow generation under changing environment in a small forested headwater catchment

Sun Haotian

Kyushu University

2017

Abstract

Headwaters contribute a substantial part of the flow in river networks. Clarification of the runoff characteristics in headwater catchments is of great importance to water resource management and disaster control. There have been many studies on runoff characteristics concerning spatial water yield, and temporal streamflow generation. However, there have been few studies that combined them to explore spatio-temporal streamflow generation. Therefore, the streamflow generation mechanisms in headwater catchments have not been fully understood. In addition to streamflow generation processes, detailed rainfall-runoff characteristics should be clarified, because previous studies mainly focused on event peak flow, despite that headwater catchments can generate multiple flow peaks during rain events directly responding to rainfall. Only examining event peak flow may neglect important rainfall-runoff characteristics in headwater catchments.

In recent years, on top of global warming and precipitation change brought by climate change, Land Use Change-Land Cover Change-Land Management Change (LUC-LCC-LMC) has been changing runoff characteristics. Therefore, understanding streamflow generation in headwater catchment under changing environment is becoming a pressing issue. Forest thinning is one of the most influential artificial changing environments that can potentially increase water yield in headwater catchments. Widely conducted in plantation forests across the world, thinning, originally aimed at increasing tree growth, has emerged as a forest management tool to prevent environmental problems, such as erosion and floods. However, the effects of thinning on runoff characteristics are not fulling understood.

The overall objective of this study is to understand the spatio-temporal streamflow generation mechanisms and rainfall-runoff characteristics under changing environment in forested headwater catchment. To achieve this objective, the following questions need to be answered: How is the spatio-temporal streamflow generation mechanism in a headwater catchment before and after forest thinning; how do the rainfall-runoff characteristics change after forest thinning?

This research was conducted during 2010-2013, at Yayama Experimental Catchment, a 2.9 ha headwater catchment underlain by porous weather granite bedrock in western Japan and covered with Cypress and Cedar tree plantation planted in 1969. Stand density was 1324 trees/ha in 2010. Thinning of 50% in tree number was conducted in 2012. Data from 2011, before thinning, and 2013, after thinning was analyzed. Annual precipitation is close to 2300 mm in each analyzed year. The similar precipitation during the monitoring period and the years before enables us to perform analysis.

To answer the first question, the relationship between the spatial distribution of water yield and the streamflow generation mechanism before and after thinning need to be clarified. The

spatio-temporal variation of streamflow generation processes in YEC was examined. The time when baseflow of the upstream section exceeded that of downstream coincided with the time when the riparian groundwater switched from downwelling to upwelling. This suggested that upwelling of the riparian groundwater increased considerably in the upstream section during the wet period, resulting a shift in the relative size of baseflow between the upstream and downstream sections. The timing of fluctuations among hillslope soil moisture, hillslope groundwater and streamflow revealed that the hillslope contributed to stormflow, but this contribution was limited to the rainy season and typhoon weather. After forest thinning of 50%, the dominant streamflow generation mechanism didn't change.

To answer the second question, the effects of thinning on rainfall-runoff characteristics need to be clarified. Because 70% of events had multiple flow peaks, and 65% of the flow peaks are not event peak flow, clarifying the flow peak characteristics is of great importance to understand rainfall-runoff characteristics. The changes in rainfall-runoff characteristics were examined in the year prior to and after thinning in YEC. The magnitude of event peak flow, event quick flow, event water yield and event response time did not change after thinning. The relationships between each flow peak and the rainfall just prior to that peak were also analyzed. The increase in accumulated quick flow, flow rise and flow drop was significant after thinning. The flow drop during the falling limb of each flow peak increased and led to a lower initial flow in the subsequent peak resulting in no increase in peak size. Significant changes were detected during large rainfall amounts after thinning. No changes were revealed in event based analysis, but the changes in flow peaks were detected, which suggested the importance of examining all flow peaks when investigating the rainfall-runoff characteristics.

Overall, the spatial variation of streamflow generation in small steep headwater catchments is closely related to hillslope groundwater and subsurface flow dynamics. Even removal of 50% trees didn't change the dominant streamflow generation mechanism and rainfall-runoff characteristics. During early post-thinning years, however, attention is needed from forest management and disaster control, because of changes in flow peaks during large rainfall events.

Contents

List of Tables

List of Figures

List of Abbreviations and Acronyms

ASI Antecedent Soil Moisture Index

D Installation depth of soil moisture sensor

G_{up} Upstream weir

G_{mid} Midstream weir

G_{down} Downstream weir

$H_{r17.5}$ Hillslope groundwater well, which is 17.5 m deep

$H_{r3.0}$ Riparian groundwater well, which is 3.0 m deep

$H_{r20.0}$ Riparian groundwater well, which is 20.0 m deep

LHG Lateral Hydraulic Gradient

θ Volumetric soil water content

VHG Vertical Hydraulic Gradient

YEC Yayama Experimental Catchment

Chapter 1

Introduction

1.1 Background

Headwater catchment can be found in the steepest portion of montane channel networks. However, there hasn't been a generally accepted definition of headwater catchment. Granted, one simple definition wouldn't be enough. Headwater catchment was defined as first-order and second-order channels by Strahler (1957) in the Horton-Strahler channel ordering system. This classification method is based on map analysis which limits its accuracy because of the map resolution (Benda et al., 2005). Another method is based on hydrological and geomorphological processes (Hack and Goodlett, 1960; Hack, 1965), which divides a headwater catchment into four zones: slopes; zero-order basins; transitional channels between zero-order basins and first-order stream (ephemeral or temporal); and first-order and second-order streams. The term "zero-order basin" represents the unchanneled and intermittent swales (Tsukamoto, 1973).

More recently, headwater catchments are defined as catchment of which the streamflow generation is controlled by runoff production at the hillslope scale (Burt, 1992). Classified by catchment area, Woods et al. (1995) suggested that the largest drainage area of headwater catchments is likely 1 km^2. The author pointed out that hydrological process of a catchment that has an area less than 1 km^2 are mainly controlled by hillslope hydrological processes, which is related to the soil depth, hillslope topography, bedrock topography and vegetation. Whereas routing processes and the structure and extent of the floodplain would influence the hydrological processes in catchments larger than 1 km^2. However, other researchers suggested that the process based classification method is more important for the headwater catchments than simply defining them by catchment area (Whiting and Bradley, 1993; Montgomery, 1999).

Headwater system contains complicated hydrologic, geomorphic, and biological processes, which have been studied for the last 60 years (Hack and Goodlett, 1960; Hewlett and Hibbert, 1967; Likens et al., 1977). Headwater catchments are important in its contribution to the discharge of mid to large scale rivers. Alexander (2007) synthesized existing watershed studies in northeastern U.S. streams, and found that first-order streams output approximately 70% of the second-order mean-annual water

volume. With a monotonic decline from headwaters to high-order streams, the contribution of 1st-order stream dropped only marginally to about 55% in fourth- and higher-order streams (Alexander, 2007).

In addition to the quantity of water, headwater catchments are also sources of sediment, fine and coarse organic matter, and nutrients (Alexander et al., 2007; Gomi et al., 2002; Morley et al., 2011; Uchida et al., 2003). Sediment movement, which can be temporarily stored in or along the streambed, banks, terraces, and debris fans in headwater catchments, may appear as sediment waves through channel networks from headwater to downstream systems (Benda and Dunne 1997a; Benda and Dunne 1997b). Kiffney et al. (2000) reported that 70% to 90% of the coarse particulate organic matter generated in headwater streams is transported downstream. The author also pointed out the amount and seasonal variation of coarse particulate organic matter and fine particulate organic matter export to downstream reaches can be controlled by types of vegetation (deciduous and coniferous) in headwater catchments (Kiffney et al. 2000). By quantifying nutrients transport of headwater catchments to downstream, Alexander (2007) found that headwater catchments contribute 65% of the nitrogen flux in the second-order stream, and this contribution declined to 40% in the fourth- and higher-order streams.

1.2 Current status on streamflow generation study

Early studies of streamflow generation focused on the visible part of the catchment during events. Abdul and Gillham (1984) found that under laboratory experiments design, when the zone of tension saturation extends to, or near, ground surface, applied rainfall can cause an immediate rise in the water table.

Though researchers in hydrology has made calls to improve communication between experimentalist and modeler (Seibert and McDonnell, 2002), there has been a movement away from field experiments and towards more complete dependence on modeling (Kirkby, 2004). Granted that computing power has become less expensive and the cost and risk of field experiment are higher compared to the former. However, there remains many fundamentals waiting for field hydrologist to explore regarding to how water cycles in catchments and reaches to streams (Barthold and Woods, 2015). As

stream gauging stations around the world are declining (Shiklomanov et al., 2002), the urge to uncover new understanding about the catchments systems are also declining (Wagener et al., 2010). Therefore, field hydrologists are calling to revisit the fields and change the amount and nature of field studies to strengthen or even break the know paradigm (Burt and McDonnell, 2015).

Streamflow generation mechanism has been studied mainly at hillslope and catchment scale over the past decades. At hillslope scale, streamflow generation is controlled by various factors such as subsurface structure, surface topography, soil, and vegetation.

Shallow subsurface flow has caught the researchers' attention since the classic experiments from Hewlett and Hibbert (1963). The generation of subsurface flow has been studied by collecting the near-surface downslope flows in troughs (Dunne and Black, 1970; Atkinson, 1978). Subsurface flow generated by subsurface structures including bedrock fissures and hollows, which provide preferential pathways, influence stormflow (Anderson and Burt 1978, Freer et al., 2002). McDonnell (1990) detected hillslope hollow drainage into the first-order channels by subsurface flow during large storms in the Maimai (M8) catchment, New Zealand. Rapid subsurface flow response through soil macropores in shallow soil (B horizon) was found in a 7.7 ha catchment, US, and the estimated subsurface flow contribution was from 1 to 48 percent of quickflow (Turton et al., 1992). In Hitachi Ohta Experimental Watershed, Japan, the subsurface flow contribution increased when flow path in upslope area was activated (Tsuboyama et al., 1994).

Surface topography such as hillslope steepness in mountainous catchments can affect streamflow (Harr 1977; McDonnell 1990). On steep hillslopes, stormflow is quickly generated by rapid flow over steep slopes (Anderson et al., 1997). Surface topography, such as hillslope spurs and hollows, exerts a strong control on soil moisture distribution in forested catchments (Burt and Butcher, 1985). Dunn et al. (1975) found that the steep slope with deep soil showed smaller saturated area during storms than the gentle slope with shallow soil in a 24 ha headwater catchment. Topography was used along with a wetness parameter to predict the saturated area and storm runoff in a 97.5 ha headwater catchment (O'Loughlin, 1986).

Soils dominated by preferential flow paths can control the timing and transfer of mobile water during rainfall events (Weiler and Naef, 2003; Weiler and McDonnell, 2007). Hoover and Hursh (1943) showed that soil depth along with topography, and hydrologic characteristics associated with different elevations influenced stormflow. By measuring the water content and matric potential, macropore flow through earthworm channel was found to contribute to streamflow generation on a gentle hillslope (Weiler and Naef, 2003). Soil with low water content and low macropore density produce infiltration excess overland flow and contribute to stream during storms (Weiler, 2001).

Vegetation types influence precipitation input patterns and soil moisture (Bachmair et al., 2012; Burke and Kasahara, 2011; Gomi et al., 2010; Jost et al., 2012). Wainwright et al. (2000) found that compared to grassland, shrubland generated more overland flow, which is responsible for a higher overall erosion rates. Afforestation and deforestation bring changes in forest stand density, which influence streamflow generation mechanism (Bosch and Hewlett, 1982; Hornbeck *et al.*, 1993; Stednick, 1996; Andréassian, 2004; Guillemette *et al.*, 2005). These changes can be evident both in inter-annual time or seasonal time scale (Bosch and Hewlett, 1982; Andréassian, 2004).

As studies were extended to catchment scale, new factors became dominant such as large structural elements, landscape organization, shifts of geology, and stream characteristics, which had stronger influences than factors at hillslope scale. Large structural elements such as size of the contributing area and storage were used to predict stormflow generation (Beven and Kirkby 1979). Jencso et al. (2009) showed that hillslope–riparian–stream water table connectivity can be a function of contributing area, where large contributing areas cause continuous connection, while small ones lead to transient connections. Connectivity may change during the year in response to the seasonal cycle of soil moisture (Western et al., 2001).

Landscape organization such as sub-catchment size was correlated with mean residence time of baseflow (McGlynn *et al*., 2003). In a 280-ha catchment at Maimai, New Zealand, landscape topography and the organization of hillslope and riparian landscape elements was linked to the riparian water table dynamics, hillslope runoff contributions and total runoff (McGlynn et al., 2004). Jencso et al. (2009) found that the

frequency of different Hillslope-Riparian-Stream connectivity durations across the watershed dominated the runoff generation in a nested 22.8 km^2 Tenderfoot Creek Catchment, USA.

When a catchment contains different types of bedrock that has different flow paths, streamflow generation also changes. The shift of geology from sandstone to granite-gneiss in the midstream reach increased deeper flow paths and discharge water downstream (Payn *et al*., 2012). Stream characteristics (e.g., river incision, drainage density, and hydraulic conductivity) were also found to improve prediction of streamflow generation (Bloomfield *et al*., 2011).

There have been many studies focus on streamflow generation. Some focused on spatial water yield pattern, while others focused on temporal streamflow generation (Ragan 1968; Dunne and Black, 1970a; Dunne and Black, 1970b; McDonnell 2003). However, there have been few studies combining these two and focusing on spatio-temporal streamflow generation (Jensco et al., 2009; Jensco and McGlynn, 2011; Payn *et al*., 2012).

Previous studies on the effect of thinning on rainfall-runoff processes have tended to examine only the characteristics of event peak flow, which is the highest peak of any one event (Wright et al., 1990; Ruprecht et al., 1991; Grace et al., 2003; Rahman et al., 2005; Dung et al., 2012a; Choi et al., 2013). However, headwater catchments generally generate multiple flow peaks, directly responding to rainfall even during a single event; while down-stream larger catchments do not (McGlynn et al., 2004; Davies and Beven, 2015). Therefore, investigating all the flow peaks in headwater catchments is important to understanding changes in rainfall-runoff processes after thinning. This information provides deeper insights to the considerable effects of rainfall on sediment transport (Warburon 2010), nutrient transport (Alexander et al., 2007), and stream morphology (Beschta and Platts, 1986).

1.3 Changing Environment

In recent years, global warming, and climate change, land cover change due to anthropogenic factors have been influencing runoff characteristics (Liu et al., 2012;

Bronstert et al., 2002). Thus predicting changes of runoff characteristics under changing environment is an urgent task. Forest thinning is one of the most influential changing environments that can potentially increase water yield in headwater catchments. Thus we use thinning as a tool to conduct our study.

Streamflow generation in headwater catchments can be altered by forest thinning by affecting evapotranspiration, soil infiltration capacity, and surface and subsurface flow paths. In Japan, about 68% of the land surface is covered by forests on steep mountains (National Astronomical Observatory). Coniferous plantations, consisting largely of Japanese cypress and cedar, account for approximately 40% of this forested area (National Astronomical Observatory). It has been suggested that the decline in forest management over the past 30 years, linked to a recession-beleaguered forestry industry, has led to an increase in flood risk and soil erosion (Japan Forestry Agency; Onda 2010). Because of the sparse understory vegetation beneath a dense canopy in abandoned plantations, soil erosion and overland flow on hillslopes can easily occur (Sidle et al., 2007; Nanko et al., 2008; Gomi et al., 2010; Miura et al., 2010). As the area of abandoned or non-managed plantation forest increases, thinning to increase tree growth (Lesch et al., 1997) has emerged as a forest management tool to prevent environmental problems, such as erosion and floods (Onda 2010). After thinning, improved light conditions under the forest canopy can increase the growth of understory vegetation (Yanai et al., 1998). This growth can improve forest floor conditions by altering infiltration capacities and potential for shallow flow pathways (Grace et al., 2006). However, findings regarding changes in event flow characteristics after thinning have been inconsistent (Wright et al., 1990; Ruprecht et al., 1991; Grace et al., 2003; Rahman et al., 2005; Dung et al., 2012a; Choi et al., 2013). Therefore, the effect of forest management on rainfall runoff characteristics in abandoned Japanese plantation forests is not fully understood (Rahman et al., 2005; Dung et al., 2012a; Dung et al., 2012b).

1.4 Objectives of this study

The overall objective of this study is to understand the spatio-temporal streamflow generation mechanisms in forested headwater catchment and address the implication of forest management on streamflow generation mechanism. To achieve this, the objective

is further divided into two objectives: understand the effects of thinning on the relationship between the spatial distribution of water yield and the streamflow generation mechanism; understand the effects of thinning on rainfall-runoff characteristics. This research was conducted at Yayama Experiment Catchment, a steep 2.98-ha headwater catchment underlain by porous weathered granite bedrock and covered with Cypress and Cedar tree plantation in western Japan planted in 1969.

The spatio-temporal streamflow generation mechanisms were examined in YEC (Chapter 2). The thinning effects on streamflow generation were examined in YEC (Chapter 3). Furthermore, the thinning effects on rainfall-runoff characteristics were examined by looking into flow peak changes after thinning in YEC (Chapter 4).

Chapter 2

Spatio-temporal streamflow generation before thinning

2.1 Introduction

Headwater streams make substantial contributions to the water yield of mid-to-large size rivers. Alexander et al. (2007) reviewed catchment studies of streams in the northeastern United States and found that first-order streams output approximately 70% of the second-order annual water yield. This contribution of first-order streams dropped only marginally in second- to fourth-order streams. Headwater can also influence downstream water quality, especially during the base flow period (Uchida *et al*., 2003; Alexander *et al*., 2007; Morley *et al*., 2011). Hence, clarification of the streamflow generation mechanism in headwater catchments is of great importance to water resource management.

Streamflow generation mechanisms have been studied mainly at the hillslope and catchment scales. At hillslope scale, streamflow generation is controlled by various factors such as subsurface structure, surface topography, soil, and vegetation. Subsurface flow generated by subsurface structures including bedrock fissures and hollows, which provide preferential pathways, influence stormflow (Anderson and Burt 1978, Freer *et al*., 2002). Surface topography such as hillslope steepness in mountainous catchments can affect streamflow (Harr 1977; McDonnell 1990). On steep hillslopes, stormflow is quickly generated by rapid flow over steep slopes (Anderson *et al.*, 1997). Soils dominated by preferential flow paths can control the timing and transfer of mobile water during rainfall events (Weiler and Naef 2003, Weiler and McDonnell 2007). Vegetation types influence precipitation input patterns and soil moisture (Bachmair *et al*., 2012; Burke and Kasahara 2011; Gomi *et al.*, 2010; Jost *et al*., 2012). Wainwright *et al.* (2000) found that compared to grassland, shrubland generated more overland flow, which is responsible for a higher overall erosion rates.

As studies were extended to catchment scale, new factors became dominant such as large structural elements, landscape organization, shifts of geology, and stream characteristics, which had stronger influences than factors at hillslope scale. Large structural elements such as size of the contributing area and storage were used to predict stormflow generation (Beven and Kirkby 1979). Landscape organization such as sub-catchment size was correlated with mean residence time of baseflow (McGlynn *et al*., 2003). The shift of geology from sandstone to granite-gneiss in the midstream reach

increased deeper flow paths and discharge water downstream (Payn *et al*., 2012). Stream characteristics (e.g., river incision, drainage density, and hydraulic conductivity) were also found to improve prediction of streamflow generation (Bloomfield *et al*., 2011).

Bedrock dominated runoff generation processes that have been recently identified at hillslope scale have yet to be incorporated into catchment scale hydrologic models (McDonnell 2003). This is because catchment scale studies commonly ignore spatial variability within a watershed (Uchida *et al.*, 2005). Thus, there is a gap in understanding of streamflow generation processes between hillslope and catchment scales. This gap prevents further understanding of the spatial variation of streamflow generation (Payn *et al.*, 2012). Recent studies have drawn attention to closing this gap (Jencso *et al*., 2009). Spatial patterns in stream discharge along valleys have revealed spatial differences in streamflow generation, which may help link hillslope scale and catchment scale processes (Payn *et al.*, 2012). However, there have been few studies focused on seasonality of the water yield pattern and the related streamflow generation mechanisms (Beven 2006; Payn *et al.*, 2012; Penna *et al.*, 2015). Tracer injection techniques have shown patterns of spatial discharge variability that can be used to understand streamflow generation from hillslope to catchment scale. However, this method consists of one-time only measurement. Accordingly, development of methods for continuous monitoring of spatial variations in streamflow can provide further insight (Botter *et al*., 2008; Barthold *et al*., 2010; Payn *et al*., 2012).

To better understand the relationship between the spatial distribution of water yield and the streamflow generation mechanism, we investigated seasonal streamflow patterns in a small, steep headwater catchment in western Japan. We monitored stream discharge at three locations, the groundwater table, and hillslope soil moisture to elucidate spatial variation of the streamflow generation mechanism. The specific objectives of the study were to (1) identify seasonal patterns in spatial variation of water yield and (2) explain spatial differences in the streamflow generation mechanism. The results provide useful information for linking hillslope and catchment hydrology in headwater catchments and provide insight into spatio-temporal differences in streamflow generation processes within small, steep headwater catchments.

2.2 Site description

The study site (Yayama Experimental Catchment (YEC)) is a 2.98-ha headwater catchment in Fukuoka Prefecture on Japan's Kyushu Island. The site is at 33°30′N and 130°39′E (Figure 2.1), and the elevation ranges from 305 to 406 m a.s.l. Mean annual precipitation from 1981 to 2000 in this region was 2098 mm (± 387 mm) based on data from Uchino meteorological station (33°32′N, 130°38′E; 80 m a.s.l.), the nearest meteorological station, which is maintained by the Ministry of Land, Infrastructure, Transport and Tourism. The entire catchment is composed of steep hillslopes and a narrow valley floor. The mean hillslope gradient is 0.81 m/m and mean stream gradient 0.37 m/m. The valley topography showed that the longitudinal gradient steepened toward the downstream portion of the catchment (Figure 2.1). Within the study reach, the substrate changed from sandy in the upstream reach to a bedrock and boulder bed with steep channel gradient in the downstream portion. The channel became incised in the section from the midstream to downstream gauge. From transects measured at each section, the depth of incision was 0.17 m at upstream, 0.83 m at midstream, and 1.69 m at downstream. The geology of the YEC is weathered granite. Thickness of the weathered granite is 13.7 m in the riparian area and 17.5 m on the hillslope, according to a drilling company field survey. Four distinct soil layers within the catchment are classified in the Dixfield–Marlow–Brayton general soil association. Japanese cypress (*Chamaecyparis obtusa* Sieb. et Zucc.) and Japanese cedar (*Cryptomeria japonica* D. Don) that were planted in 1969 cover the catchment. The cypress comprises 67% of all trees, and the cedar accounts for the remaining 33%.

2.3 Methods

This study was carried out from January to December 2011. It was designed to monitor streamflow at multiple locations in the catchment and to explain spatio-temporal water yield variation using precipitation, groundwater elevation, soil moisture, and soil water potential measured on the hillslope and in the riparian zone.

Three stream gauge stations were installed. The upstream gauge (G_{up}) was immediately downstream of where the stream starts during the dry season. The

midstream gauge (G_{mid}) was above where the stream gradient becomes steep, and the downstream gauge (G_{down}) was at the catchment outlet (Figure 2.1). The difference in elevation from G_{up} to G_{mid} was 21.8 m with a gradient of 0.25 m/m, and 32.9 m with a gradient of 0.55 m/m from G_{mid} to G_{down}. Each station consisted of a V-notch gauge and a Parshall flume. The V-notch gauge was used to monitor baseflow and the Parshall flume the stormflow. The stage was monitored at 10-min intervals by the V-notch and 5-min intervals by the Parshall flume, using a WT-HR water level logger (TruTrack, Christchurch, New Zealand). Stage sensor readings were checked weekly with visual stage readings from June through July (wet period) and twice per month during the rest of the year to corroborate continuous measurements. Water yield among the three gauge sites was also compared.

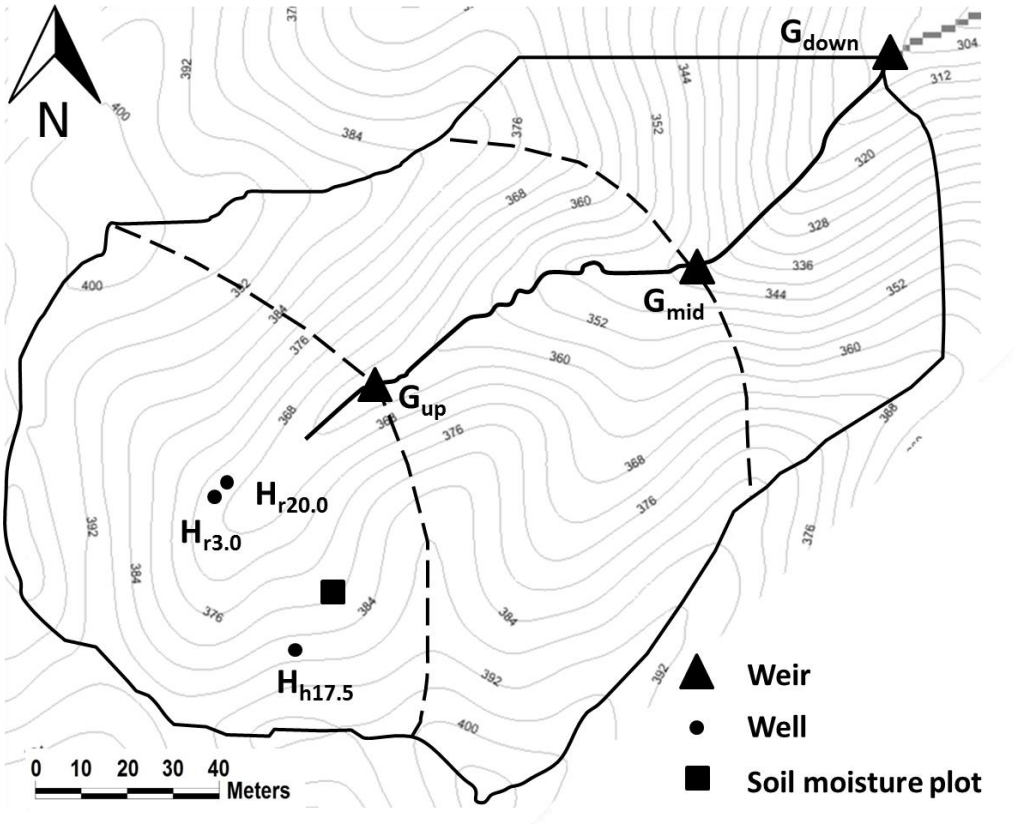

Fig. 2.1 Map of the study site in the Yayama Experimental Catchment (YEC) G_{up}, G_{mid} and G_{down} are the gauges; $H_{r3.0}$, $H_{r20.0}$, $H_{h17.5}$ are the groundwater wells. The dashed lines are for sub-catchment division. Contour interval is 4 m.

Precipitation was recorded at the weather station located 320 m from the center of the catchment, at an elevation of 390 m. A 0.5-mm tipping bucket rain gauge (TK-1; Takeda Keiki, Tokyo) was used, and the data were collected at an interval of 10 min.

Long-term precipitation data were acquired from the nearby Uchino meteorological station.

Groundwater level was monitored on the hillslope and in the riparian zone. A hillslope well ($H_{h17.5}$) was located upslope and installed to a depth of 17.5 m from the surface (Figure 2.1). Two wells of different depths were installed at the same location in the riparian zone to observe the vertical head gradient (VHG). A deep riparian well ($H_{r20.0}$) was installed to a depth of 20 m, with a screen present from 4 to 20 m. A shallow riparian well ($H_{r3.0}$) was installed to a depth of 3 m, with a screen present from 1 to 3 m. Elevation and horizontal distance between the ground locations of $H_{h17.5}$ and H_{r20} were 15.2 and 36.6 m, respectively. Water level fluctuation in each well was recorded with a Hobo U20 water level data logger (Onset Company, Bourne, MA, USA) at 10-min intervals. Manual measurements of groundwater levels in each well were conducted twice per month to check sensor readings. The VHG between $H_{r20.0}$ and $H_{r3.0}$ was calculated by

$$\mathrm{VHG}=\Delta h_1/l_1\,, \tag{2.1}$$

where Δh_1 is the head difference between $H_{r20.0}$ and $H_{r3.0}$ and l_1 is the horizontal distance between them.

The lateral head gradient (LHG) between $H_{h17.5}$ and $H_{r3.0}$ was calculated by

$$\mathrm{LHG}=\Delta h_2/l_2, \tag{2.2}$$

where Δh_2 is the head difference between $H_{h17.5}$ and $H_{r3.0}$ and l_2 is the horizontal distance between them.

Soil moisture was continuously monitored at three locations in the same hillslope area. The sampling locations were 5 m apart and 14.8 m upslope from Gup (Figure 2.1). Each sampling station contained three soil moisture sensors (EC-5; Decagon Devices Inc., WA, USA) and three tensiometers (DIK-3042; Daiki Rika Kogyo Co., Ltd, Japan) at three depths (10, 30, and 50 cm), which collected data at 1-h intervals. The soil moisture was calculated using the soil samples excavated from 3 soil pits on the hillslope where the soil moisture plot is located. The antecedent soil moisture index (ASI) (Haga et al.,

2005) was calculated for each storm event as initial storage of the surface soil layer in the catchment, based on the volumetric water content at the measurement points:

$$\mathrm{ASI} = \theta \times D, \tag{2.3}$$

where θ is the volumetric average soil water content (m^3/m^3) at depth of 0.1 m, 0.3 m and 0.5 m and D is the installation depth (0.5 m).

To identify differences of medians between pairs of water yield data in the same period, the Mann–Whitney U test was used (Iman and Conover 1983). The Kruskal–Wallis test was used to determine any significant overall differences among the three groups of water yield data in the same period (Iman and Conover 1983). This test has the advantage of not requiring normality nor equal variances of data.

2.4 Results and discussion

2.4.1 Temporal and spatial water yield pattern

The 2011 annual precipitation measured in the YEC was 2469 mm. The mean annual precipitation from 1981 to 2011 at the nearby Uchino weather station was 2098 mm (± 387 mm), whereas it was 2632 and 2397 mm in 2010 and 2011, respectively. These data show that the study year and year prior were relatively wet years in the region. Precipitation falls occasionally as snow in January and February, and then melts in early February.

The hydrograph of water yield showed various patterns among the three gauging stations (Figure 2.2a). We divided the year into three periods based on the hyeto-hydrograph (Figure 2.2a). The dry period was January through late May when the water yield was low and relatively stable. The wet period was from the first major event recorded in late May through the end of the rainy season in mid-July, when the water yield continuously increased. The dry-down period was from mid-July through December, when the water yield slowly declined.

During the dry period, the water yield ranked in the order of G_{down}, G_{mid}, and G_{up}. However, values were similar among the three stations: all < 0.1 mm/h (Table 2.1). During the wet period, the water yield increased at each gauge site, and differences of

water yield among the three gauges widened. Additionally, the water yield at G_{mid} did not increase as much as at the other gauges, with 0.185 mm/h on average and the smallest standard deviation (Table 2.1). Large differences in water yield between G_{mid} and the other gauges persisted for the remainder of the year. Water yield at G_{up} showed a slower increase than G_{down} at the beginning of the wet period but surpassed that of G_{down} in July. During the dry-down period, the difference in water yield between these gauges decreased, but G_{up} maintained larger values than G_{down} through December (Table 2.1 and Figure 2.2a). The water yields in the same period from different gauges were significantly different (Kruskal–Wallis test, $p = 0.000$ for all groups). Also, all combinations of two groups of water yield in the same period had significantly different medians (Mann–Whitney test).

Table 2.1. The statistical summary of water yield at each gauge in each period (sum, average, standard deviation, interquartile range and maximum-minimum).

		Down	Mid	Up
Sum (mm)	Dry	189.1	47.0	85.1
	Wet	546.9	226.9	450.2
	Dry-down	874.3	189.6	967.7
Average (mm/h)	Dry	0.056	0.014	0.025
	Wet	0.447	0.185	0.368
	Dry-down	0.212	0.096	0.234
Standard Deviation	Dry	0.057	0.019	0.016
	Wet	0.244	0.105	0.227
	Dry-down	0.107	0.068	0.116
Median (mm/h)	Dry	0.047	0.010	0.022
	Wet	0.477	0.196	0.430
	Dry-down	0.176	0.078	0.215
Interquartile Range (mm/h)	Dry	0.024	0.018	0.021
	Wet	0.368	0.179	0.377
	Dry-down	0.101	0.090	0.122
Maximum-Minimum (mm/h)	Dry	1.342	0.414	0.253
	Wet	1.985	0.633	1.548
	Dry-down	1.504	0.595	0.799

The low water yield at G_{mid} during the wet and dry-down periods may be attributed to the topography at the gauge site. Specifically, G_{mid} was immediately above where the longitudinal gradient steepened (Figure 2.1) from 0.25 to 0.55 m/m, and the substrate was sandy gravel with boulders, which is probably highly permeable. Studies of channel

morphology and stream-groundwater exchange have revealed downwelling trends upstream of steps (Wondzell *et al*., 2009), and stronger downwelling trends were associated with greater step size (Kasahara and Wondzell 2003). The slope steepened immediately downstream of G_{mid}, resulting in a head drop of 23.3 m. This may have had an effect similar to a large step, driving downwelling flow upstream of G_{mid}. The highly permeable substrate and greater water yield may have accelerated downwelling upstream of G_{mid} during the wet period, increasing the differences in water yield between G_{mid} and the other gauges.

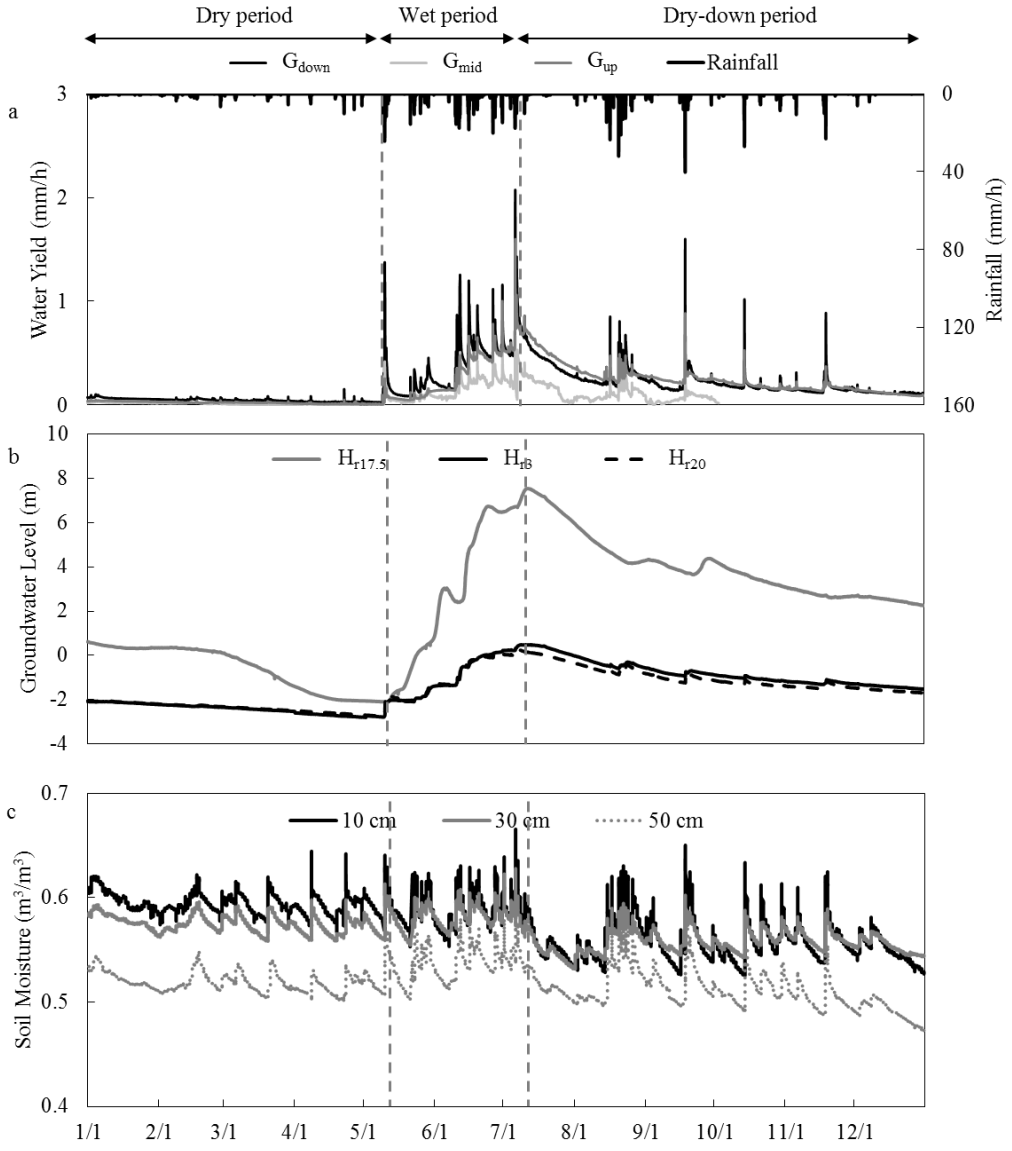

Fig. 2.2 (a) hydrograph, (b) groundwater, (c) soil moisture in 2011. The vertical dashed lines are for season division. Zero point for the y-scale in groundwater represents the ground elevation of the riparian well.

G_{up} was immediately below where the stream started, and G_{down} was where bedrock exposure was present. Water yield at the two gauges showed similar annual patterns, but their relative size switched during the wet period. Peak flow during precipitation events was consistently greater at G_{down}, but baseflow between precipitation events increased at G_{up} toward the end of the wet period (Figure 2.2a).

Several studies have examined spatial differences of water yield in headwater catchments (Jencso *et al.*, 2009; Jencso and McGlynn 2011). For example, Payn *et al*. (2012) reported a greater downstream water yield during the summer recession period in the Tenderfoot Creek Experimental Forest catchment. In the YEC, the spatial difference in water yield changed seasonally.

2.4.2 Groundwater contribution during baseflow

Hillslope groundwater showed a steady decline from January, reaching the lowest level at the beginning of May. Hillslope groundwater level rose as the rainy season began, and peaked in July. After the peak, the level gradually declined the rest of the year, except for a slight increase in response to two typhoon rain events (Figure 2.2b). The hillslope groundwater table remained within the weathered bedrock layer. Riparian groundwater levels were stable from January through May and began to increase from a rain event on May 9 that produced 226 mm of precipitation. The groundwater levels increased with each large rain event, peaking in mid-July. During the rainy season, the stream expanded upstream to the area where Hr20.0 and Hr3.0 were located, and riparian groundwater levels measured at these wells were above the valley floor surface from June 23 through July 31. Those levels declined gradually the remainder of the year, except for a slight increase in response to four typhoon rain events (Figure 2.2b). During the wet period, the riparian groundwater table could rise above the weathered bedrock layer into the soil.

When groundwater levels on the hillslope and in the riparian zone were compared, the hillslope groundwater level was always higher than the riparian groundwater level, except for a short period in May (Figure 2.2b). The range of hillslope and riparian groundwater fluctuation also differed, with the shallow riparian groundwater level

showing only a 3.2-m range of fluctuation and the hillslope groundwater level a 9.1-m range.

Figure 2.3 presents LHG values between $H_{h17.5}$ and $H_{r3.0}$. Positive values indicate that the LHG is from the hillslope to riparian zone, and negative values indicate the reverse. LHG was positive most of the year, except for one day in May. The top of the screening for wells $H_{r20.0}$ and $H_{r3.0}$ was 4 and 1 m below ground, respectively, and the groundwater level in both wells was above the screen the most of the year. Thus, we also calculated the VHG between the two riparian wells (Figure 2.3). Positive and negative values indicate upwelling and downwelling, respectively. The VHG showed a downwelling trend with relatively stable values from January through May, with fluctuations at the beginning of the wet period. Later in that period, the VHG had a steady upwelling trend, which continued through the end of the year (Figure 2.3a).

The LHG was always greater than the VHG, except for an event during May. The catchment has steep hillslopes with a narrow valley floor, and the LHG may represent the hillslope groundwater contribution to streamflow. However, this value was only calculated between two points. Compared with the VHG, the consistently greater LHG may indicate a larger contribution of lateral inflow to the stream, but the spatial variability of hydraulic conductivity in the area is not known. Some studies in zero-order catchments have also reported that lateral inflow dominated streamflow generation (Frisbee *et al*., 2007; Sidle *et al*., 2000). Additionally, studies in small granite catchments similar to the YEC reported that subsurface stormflow through the soil profile can have a dominant contribution to streamflow (Onda *et al*., 2001; Onda *et al*., 2006). The wells used to calculate LHG and VHG in our study were in the upstream portion of the catchment (Figure 2.1), so the strong lateral inflow may only be applicable to that area. However, considering that the downstream portion of the stream was incised and flowing on exposed bedrock and boulders, a larger contribution of lateral inflow than vertical upwelling may also apply to the downstream portion of the catchment.

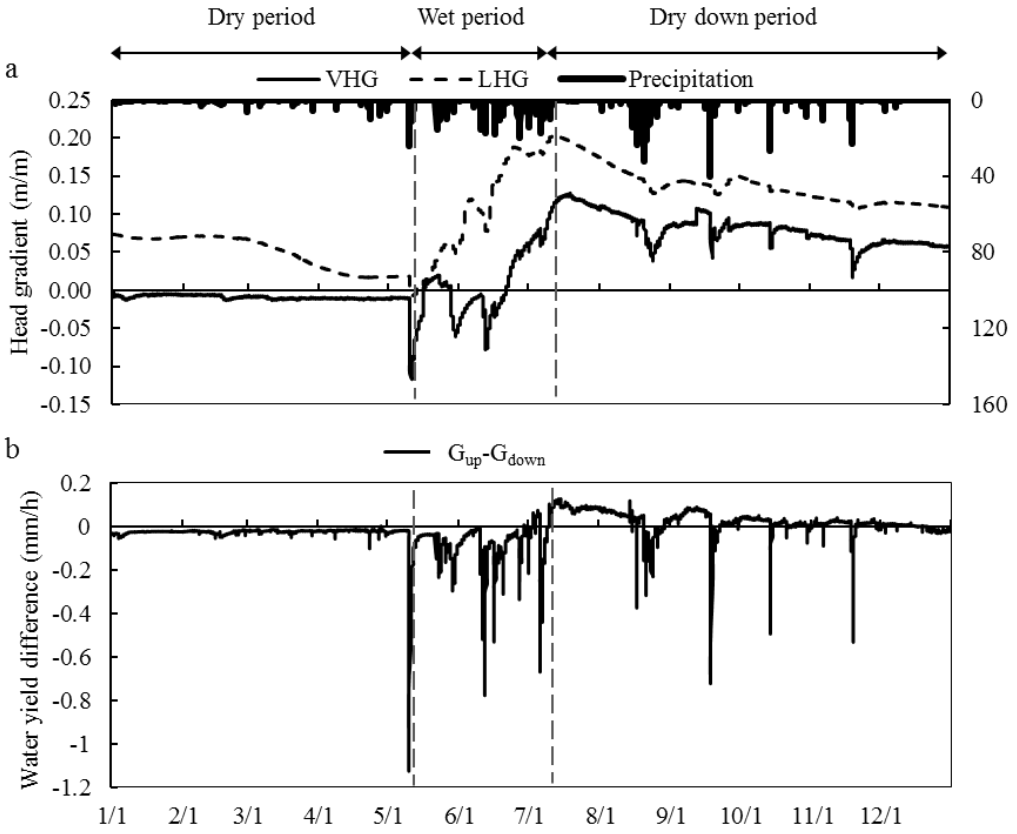

Fig. 2.3 a. Vertical hydraulic gradient (VHG) between $H_{r20.0}$ and $H_{r3.0,}$ positive values mean riparian groundwater upwelling, and negative values mean riparian groundwater downwelling; lateral hydraulic gradient (LHG) between $H_{h17.5}$ and $H_{r3.0}$, positive value means hillslope groundwater contributing to riparian groundwater, negative values mean riparian groundwater contributing to hillslope groundwater; b. Water yield difference between G_{up} and G_{down}, positive values mean $G_{up} > G_{down}$, negative values mean $G_{up} < G_{down}$.

The relative size of LHG to VHG does not explain the greater water yield at G_{up} during the wet and dry-down periods. VHG values showed that the riparian groundwater changed from downwelling to upwelling, which overlapped when the water yield at G_{up} became larger than that at G_{down} (Figure 2.3b). During the baseflow period, when VHG indicated downwelling, the water yield was $G_{up} < G_{down}$, whereas it was $G_{up} > G_{down}$ when VHG indicated upwelling. During events at the beginning of wet period, VHG showed downwelling, and the water yield difference was negative. During events at the end of the wet period and entire dry-down period, VHG indicated upwelling, while the water yield difference still had negative values. These findings suggest that in addition to lateral inflow, vertical upwelling in the riparian zone of the

zero-order basin supplied water to the upstream reach that was sufficient to switch the water yield balance between the two gauges.

Fluctuation of groundwater level has been linked to stream water yield in other studies. For instance, studies in the Sierra Nevada mountains in California USA revealed that fast stormflow response and extended recession flow were produced by fluctuations in groundwater levels that created saturated areas on hillslopes (McNamara *et al*., 1998; Yamazaki *et al*., 2006). Although we could not quantify the contributions of lateral and vertical groundwater inflow to the stream, our results show that fluctuations in groundwater levels partially explain water yield patterns in the YEC.

2.4.3 Groundwater and subsurface flow contribution during stormflow

Hillslope soil moisture has been used as an indicator of hillslope-stream connectivity and throughflow (Burke and Kasahara 2011; Moore *et al*., 2011; Penna *et al*., 2011; Fu *et al*., 2013). In the present study, we compared hillslope soil moisture to streamflow and hillslope groundwater level to explain water movement during stormflow in the YEC.

The relationship between soil moisture and water yield was examined. The results of a typical vent in dry and wet periods are plotted in Figure 2.4. For the March 20–22 event (dry period), water yield increased and peaked before the hillslope soil moisture, suggesting that the hillslope contribution to stormflow was small (Figure 2.4a left). Water yield plotted versus soil moisture shows clockwise hysteresis (Figure 2.4b left). For the event of June 30–July 1 (wet period), water yield reacted more slowly than soil moisture, and peaked after the hillslope soil moisture peak, indicating a potential hillslope contribution to stormflow (Figure 2.4a right). For this event, the plot of water yield versus soil moisture shows counter-clockwise hysteresis (Figure 2.4b right).

All precipitation events with hysteresis of soil moisture and water yield are summarized in Figure 2.5. ASI was used together with precipitation. The hysteresis relationship between hillslope soil moisture and water yield showed seasonality. Most events during the dry period had a clockwise hysteresis relationship (i.e., no hillslope contribution), whereas most events during the wet period showed counter-clockwise

hysteresis (potential hillslope contribution). During the dry-down period, clockwise hysteresis again became the dominant pattern, except for typhoon events in August that resulted in a clockwise hysteresis relationship. This indicates that subsurface flow can contribute to the stream during typhoons. These results agree with findings of hillslope contribution during rain events in the rainy season only (Onda *et al.*, 2006; Penna *et al.*, 2015). Penna *et al.* (2015) found that hillslopes delivered water to the stream during events in the rainy season. Onda *et al*. (2006) reported that shallow subsurface flow can be a major contributor to the stream in a steep granite catchment during the rainy season. A similar change of hillslope-streamflow hysteresis patterns was detected by McGuire and McDonnell (2010), who found hysteresis patterns as a result of increasing wetness conditions.

We also examined the relationship between soil moisture and hillslope groundwater level during stormflow (Figure 2.4). Specifically, the relationship between average soil moisture at 10 cm and hillslope groundwater level was compared to address recharge and discharge of hillslope groundwater. We defined the discharge condition as when the hillslope groundwater level decreases continuously despite rainfall events. The recharge condition was defined as groundwater level increase with rainfall events. In mountainous catchments, groundwater in the riparian zone tends to have a different response time as the hillslope groundwater (Seibert *et al.*, 2003). This difference can lead to hysteresis behavior between hillslope groundwater and runoff (Penna *et al.*, 2010; Penna *et al.*, 2011).

Measurement of water potential in the hillslope soil profile showed that water moved downward almost the entire study period (Figure 2.2d), suggesting that the water infiltrated into deeper layers of the soil profile in the YEC. Results from two typical events that were also used for analysis of soil moisture and water yield are plotted in Figure 2.4a. The event on March 20 had a continuous decrease of hillslope groundwater level during and after the event, suggesting that hillslope groundwater maintained a discharge trend because the precipitation amount was too small to influence the groundwater level (Figure 2.4a left). Conversely, the event on June 30 had an increasing hillslope groundwater level with decreasing soil moisture, indicating recharge of hillslope groundwater level (Figure 2.4c right).

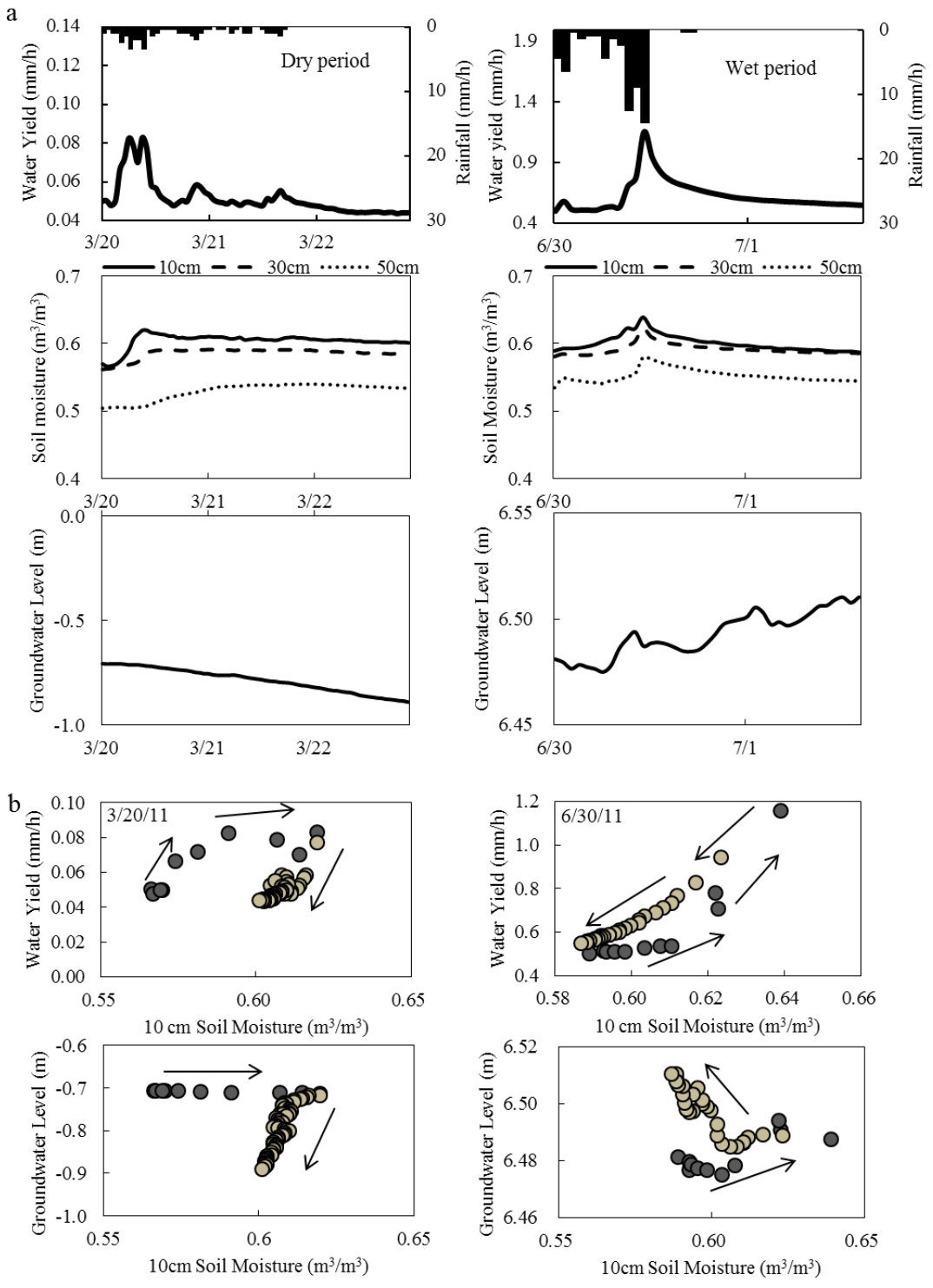

Fig. 2.4 a. Hydrograph and soil moisture and hillslope groundwater level during two events in 2011; b. 10 cm soil moisture plotted with upstream water yield for two events. Black dots represent the rising limb; light brown dots represent the falling limb.

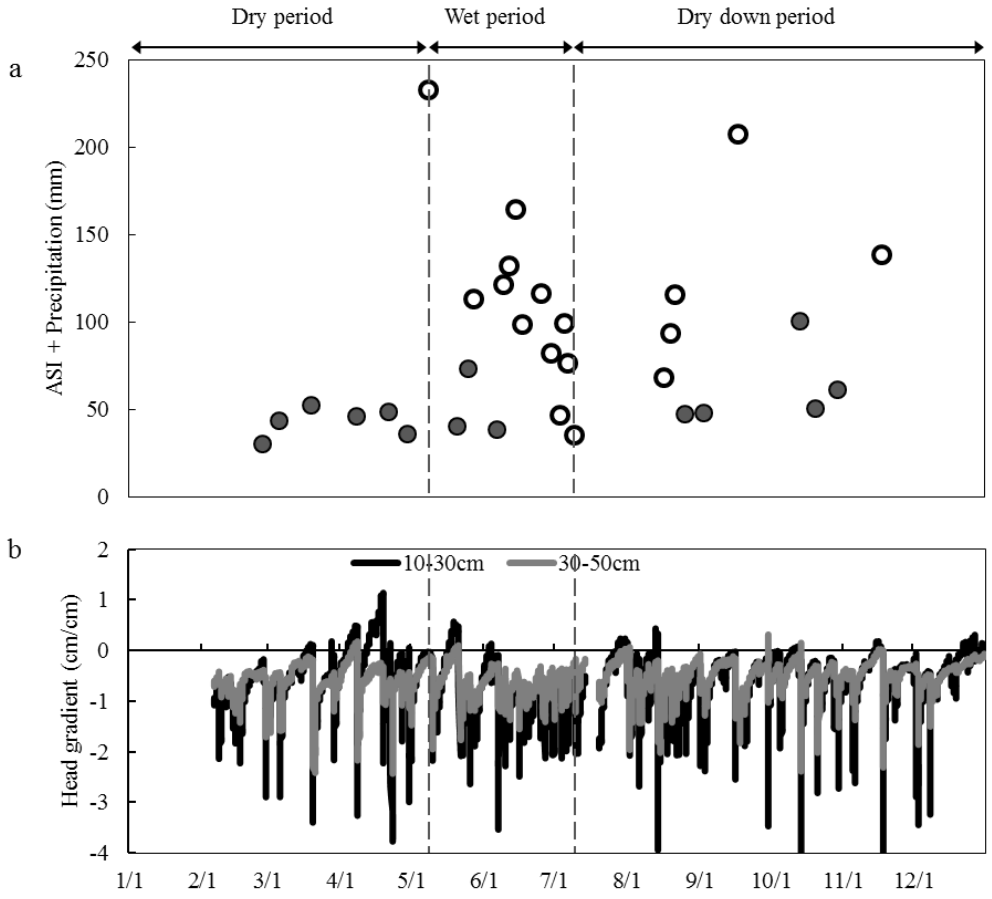

Fig. 2.5 a.Temporal evolution of rainfall + ASI for the study year. Closed circles represent clockwise hysteresis relationship between soil moisture and water yield; open circles represent counter-clockwise hysteresis relationship between soil moisture and water yield; b. soil water head gradient. The vertical dashed lines are for season division.

Recharge and discharge during the entire study period are shown in Figure 2.6. During the dry period, hillslope groundwater showed no response or slower response and peaked after soil moisture, leading to clockwise hysteresis relationship between soil moisture and hillslope groundwater. Water is retained in the hillslope, and a disconnected hillslope may not allow water to percolate deep into the hillslope groundwater, causing little or no hillslope groundwater contribution. Conversely, during events in the wet period, hillslope groundwater peaked prior to soil moisture or even continued to increase after the event, producing a counter-clockwise hysteresis relationship. During these events, a state of connection was assumed to be established within the hillslope, and water could percolate quickly into the groundwater. This caused a rapid response of hillslope groundwater, so the hillslope began to release water.

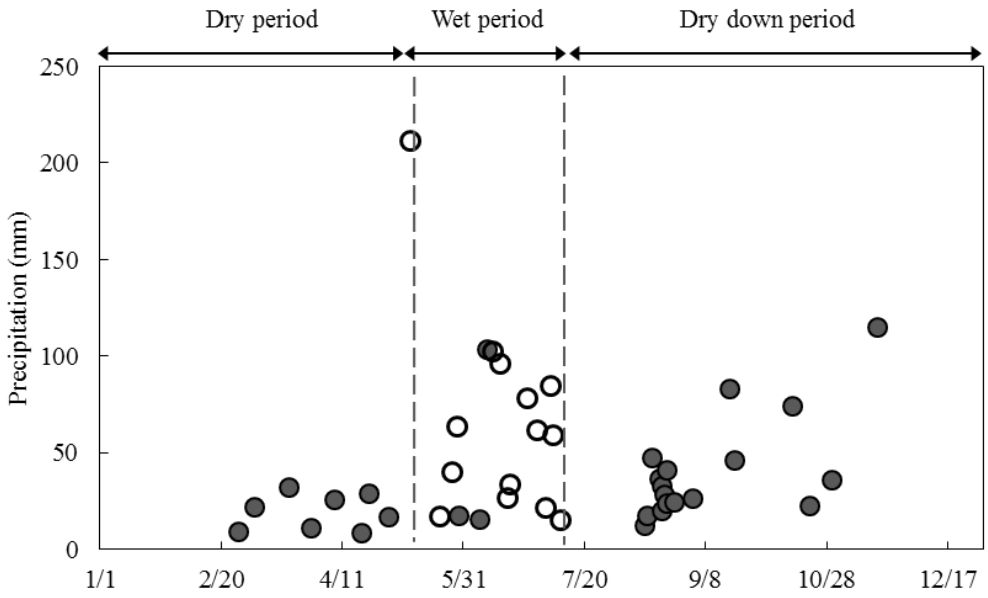

Fig. 2.6 Temporal evolution of rainfall + ASI for the study year. Closed circles represent hillslope groundwater discharge conditions, open circles represent hillslope groundwater recharge conditions. The vertical dashed lines are for season division.

Seasonal patterns of soil moisture to water yield and soil moisture to groundwater were similar (Figures 2.6 and 2.7), indicating hillslope groundwater recharge and subsurface flow during stormflow in the wet period. However, there was a short time difference. At the beginning of the wet period, hillslope groundwater was recharging while the hillslope was disconnected from the groundwater. During typhoon season, the hillslope groundwater was discharging while hillslope subsurface flow was present.

2.4.4 Streamflow generation mechanism in the YEC

The studied catchment was small but water yield varied spatially within it. Therefore, relative size of the water yield varied seasonally. In this section, we summarize the results of streamflow, groundwater, and soil moisture to elucidate streamflow generation mechanisms in the YEC.

During the dry period, water yield was low, had little variability, and increased slightly downstream. Riparian groundwater was likely a major source of streamflow, and lateral inflow from the riparian zone to stream channel dominated at all three gauge sites. Precipitation was weak and less frequent, and the response of soil moisture to stormflow was slower than that of streamflow. Precipitation did not translate to an

increase in groundwater level, suggesting disconnection of the hillslope from the stream and groundwater.

During the wet period, groundwater level and soil moisture were increased by a large amount of precipitation. In addition to lateral inflow, strong upwelling in the riparian zone of the zero-order basin increased water yield at G_{up}. The water yield at G_{mid} did not show as large an increase as at G_{up} and G_{down}, which may be attributable to the sandy permeable substrate and longitudinal gradient in the midstream reach. The upstream water yield exceeded that of downstream during the wet period. During stormflow, the response of soil moisture preceded that of streamflow, and this translated to an increase in groundwater level. This suggests that the hillslope was connected to the stream and that subsurface flow may appear during and after the rain event.

During the dry-down period, upstream water yield efficiency remained higher than that of downstream, although the water yield declined throughout the catchment. The soil moisture and the groundwater level decreased gradually with strong response to heavy rainfall events. Upstream riparian groundwater continued upwelling, and subsurface flow was generated during heavy rain from a typhoon.

A lack of downstream soil moisture and groundwater data prevented exploration of more detailed spatial variation of streamflow generation. To generalize the present results, multi-catchment comparison is needed, and the relative influences of geology and topography should be clarified (Jencso and McGlynn 2011; Richardson *et al*., 2012). However, our results provide valuable insight into the linkage between the seasonal and spatial water yield patterns and spatio-temporal differences in streamflow generation.

2.4.5 Implications

Our study highlights the importance of groundwater movement in streamflow generation. We emphasized the relationship between water yield patterns and streamflow generation. One of the typical studies of streamflow generation use a lumped model called a “tank model” that treats the catchment as vertically arranged multiple tanks with several outlets (Sugawara 1961; Sidle et al., 2011). Difficulties often arose when trying to extrapolate their results to larger catchment size.

The relationship between water yield pattern and streamflow generation is likely to be transmitted to other headwater catchments, since headwater catchments typically evolve from a gentle zero-order basin to a relatively steep valley associated with steep, incised channel morphology (Benda *et al*., 2005). Early studies used multi-gauge setup in small catchments to study the stormflow generation process, transferred to further downstream areas (Ragan 1968; Dunne and Black, 1970a; Dunne and Black, 1970b). However, seasonal variation of water yield was not clarified. In gentle catchments, there would be more groundwater inflow in areas where the regional groundwater table contributes to the stream. It remains in question whether gentle catchments show similar water yield patterns, because the streamflow generation processes may be different.

2.5 Conclusion

Spatio-temporal variations of streamflow generation in a small, steep headwater catchment were examined. Water yield in the upstream section was less than in the downstream section during the dry and wet periods, but this order changed in the subsequent dry-down period. Baseflow in the upstream section surpassed that of downstream at the end of the wet period, which coincided with the time when riparian groundwater switched from downwelling to upwelling. This suggests that the upwelling of the riparian groundwater considerably increased the upstream baseflow during the wet period, inducing a shift in relative amount of baseflow between the upstream and downstream sections. Stormflow was consistently greater in the downstream section. However, the contribution source changed seasonally. Hillslope groundwater discharge and hillslope subsurface flow greatly contributed to stormflow, but these contributions only appeared during the wet period. Overall, these results suggest that streamflow generation has a strong spatial variation even in small, steep headwater catchments, which may indicate linkage between hillslope scale and catchment scale hydrologic processes. Additional studies using more detailed soil moisture and groundwater data are needed.

2.6 Summary

Headwaters contribute a substantial part of the flow in river networks. However, spatial variations of streamflow generation processes in steep headwaters have not been well studied. In this chapter, we examined the spatio-temporal variation of streamflow generation processes in a steep 2.98-ha headwater catchment. The time when baseflow of the upstream section surpassed that of downstream was coincident with the time when riparian groundwater switched from downwelling to upwelling. This suggests that the upwelling of riparian groundwater increased considerably in the upstream section during the wet period, producing the shift in relative size of baseflow between the upstream and downstream sections. The timing of fluctuation among hillslope soil moisture, hillslope groundwater, and streamflow reveal that the hillslope contributed to stormflow, but this contribution was limited to the wet period. Overall, these results suggest that streamflow generation had strong spatial variation, even in small steep headwater catchments.

Chapter 3

Effects of thinning on spatio-temporal streamflow generation

3.1 Introduction

In recent years, global warming, and climate change, land cover change due to anthropogenic factors have been influencing runoff characteristics (Liu et al., 2012; Bronstert et al., 2002). Thus predicting changes of runoff characteristics under changing environment is an urgent task. Forest thinning is one of the most influential changing environments which induce immediate change in streamflow generation (Bosch and Hewlett, 1982; Bari et al., 1996; Andréassian, 2004). Streamflow generation in headwater catchments can be altered by forest thinning by affecting transpiration (Tateishi et al., 2015), soil infiltration capacity (Chen et al., 2014), and groundwater tables (Bari et al., 1996). Canopy transpiration decreased 44.0 and 21.2% for Japanese cypress plot and Japanese cedar plot after 50% thinning (Tateishi et al., 2015). Thinning of 30% trees in number can substantially improve soil infiltration rate and water storage capacity of pine-oak mixed forest in Qinling Mountains, China (Chen et al., 2014). Forest thinning resulted in an increase in groundwater levels and subsequently groundwater discharge area in Western Australia (Bari et al., 1996). However, spatial variations of streamflow generation processes in steep headwaters after thinning have not been well studied (Andréassian, 2004; Penna et al., 2011).

Mountainous catchment streamflow responses to rainfall events are often dominated by a combination of lateral subsurface flows and saturated overland flow (Buttle and McDonald, 2002; Freer et al., 2002; McGuire et al., 2005; Weiler and McDonnell, 2007; Zillgens et al., 2007). Thresholds as one of the non-linear behaviours commonly exist in hydrologic and geomorphic system, occurring at different levels of complexity (Zehe and Sivapalan, 2009). When a catchment exceeds thresholds, water movement becomes more efficient (Zehe and Sivapalan, 2009). Various researches have showed that subsurface stormflow is an intermittent phenomenon which occurs when a catchment receives a threshold of rainfall amount (Whipkey 1965; Mosley, 1979; Haga et al., 2005; Tromp-van-Meerveld and McDonnell, 2006).

Previous studies found that lateral subsurface flow is controlled by subsurface topography, lateral subsurface structures or bedrock topography. Beven and Kirkby (1979) found that for shallow permeable soils, when bedrock topography might be

assumed to be parallel to the surface, transmissivity and surface topography are the first order controls for saturated overland flow and subsurface flow. Built on this fundamental insight was the TOPMODEL concept (Beven and Kirkby, 1979). Tromp-van-Meerveld et al. (2006) used the concept of fill and spill mechanism to explain bedrock control on a hillslope plot where threshold behavior of subsurface stormflow was observed. Woods et al. (1995) pointed out that hydrological process of a catchment that has an area less than 1 km^2 are mainly controlled by hillslope hydrological processes, which is related to the soil depth, hillslope topography, bedrock topography and vegetation.

Hillslope soil moisture has been used as an indicator of hillslope-stream connectivity and throughflow (Burke and Kasahara 2011; Moore *et al*., 2011; Penna *et al*., 2011; Fu *et al*., 2013). Penna *et al.* (2015) found that hillslopes delivered water to the stream during events in the rainy season. Onda *et al*. (2006) reported that shallow subsurface flow can be a major contributor to the stream in a steep granite catchment during the rainy season. Changes of hillslope-streamflow hysteresis patterns was detected by McGuire and McDonnell (2010), who found hysteresis patterns as a result of increasing wetness conditions. In YEC, hysteresis patterns and shallow subsurface flows were identified during rainy season and typhoon weather (Sun et al., 2017).

The spatio-temporal streamflow generation mechanisms before thinning were identified in the second chapter. The objective of this study is to examine thinning effects on spatio-temporal streamflow generation mechanisms. We first examined whether there were any changes in streamflow generation after thinning. We then further investigated the spatial variation in streamflow generation (both longitudinally and hillslope) after thinning. We monitored stream discharge at three locations, the groundwater table, and hillslope soil moisture at three transect across the catchment.

3.2 Materials and Methods

3.2.1 Site description

The study site (Yayama Experimental Catchment (YEC)) is a 2.98-ha headwater catchment in Fukuoka Prefecture on Japan's Kyushu Island. The site is at 33°30′N and

130°39′E (Figure 3.1), and the elevation ranges from 305 to 406 m a.s.l. Mean annual precipitation from 1981 to 2000 in this region was 2098 mm (± 387 mm) based on data from Uchino meteorological station (33°32′N, 130°38′E; 80 m a.s.l.), the nearest meteorological station, which is maintained by the Ministry of Land, Infrastructure, Transport and Tourism. The entire catchment is composed of steep hillslopes and a narrow valley floor. The mean hillslope gradient is 0.81 m/m and mean stream gradient 0.37 m/m. The valley topography showed that the longitudinal gradient steepened toward the downstream portion of the catchment (Figure 3.1). Within the study reach, the substrate changed from sandy in the upstream reach to a bedrock and boulder bed with steep channel gradient in the downstream portion. The channel became incised in the section from the midstream to downstream gauge. From transects measured at each section, the depth of incision was 0.17 m at upstream, 0.83 m at midstream, and 1.69 m at downstream. The geology of the YEC is weathered granite. Thickness of the weathered granite is 13.7 m in the riparian area and 17.5 m on the hillslope, according to a drilling company field survey. Four distinct soil layers within the catchment are classified in the Dixfield–Marlow–Brayton general soil association. Japanese cypress (Chamaecyparis obtusa Sieb. et Zucc.) and Japanese cedar (Cryptomeria japonica D. Don) that were planted in 1969 cover the catchment. The cypress comprises 67% of all trees, and the cedar accounts for the remaining 33%. Thinning of 50% in tree number were perform during January to March, 2012.

3.2.2 Methods

Precipitation was recorded at the weather station located 320 m from the center of the catchment, at an elevation of 390 m. A 0.5-mm tipping bucket rain gauge (TK-1; Takeda Keiki, Tokyo) was used, and the data were collected at an interval of 10 min. Long-term precipitation data were acquired from the nearby Uchino meteorological station.

Three stream gauge stations were installed. The upstream gauge (G_{up}) was immediately downstream of where the stream starts during the dry season. The midstream gauge (G_{mid}) was above where the stream gradient becomes steep, and the downstream gauge (G_{down}) was at the catchment outlet (Figure 3.1). The difference in

elevation from G_{up} to G_{mid} was 21.8 m with a gradient of 0.25 m/m, and 32.9 m with a gradient of 0.55 m/m from G_{mid} to G_{down}. Each station consisted of a V-notch gauge and a Parshall flume. The V-notch gauge was used to monitor baseflow and the Parshall flume the stormflow. The stage was monitored at 10-min intervals by the V-notch and 5-min intervals by the Parshall flume, using a WT-HR water level logger (TruTrack, Christchurch, New Zealand). Stage sensor readings were checked weekly with visual stage readings from June through July (wet period) and twice per month during the rest of the year to corroborate continuous measurements.

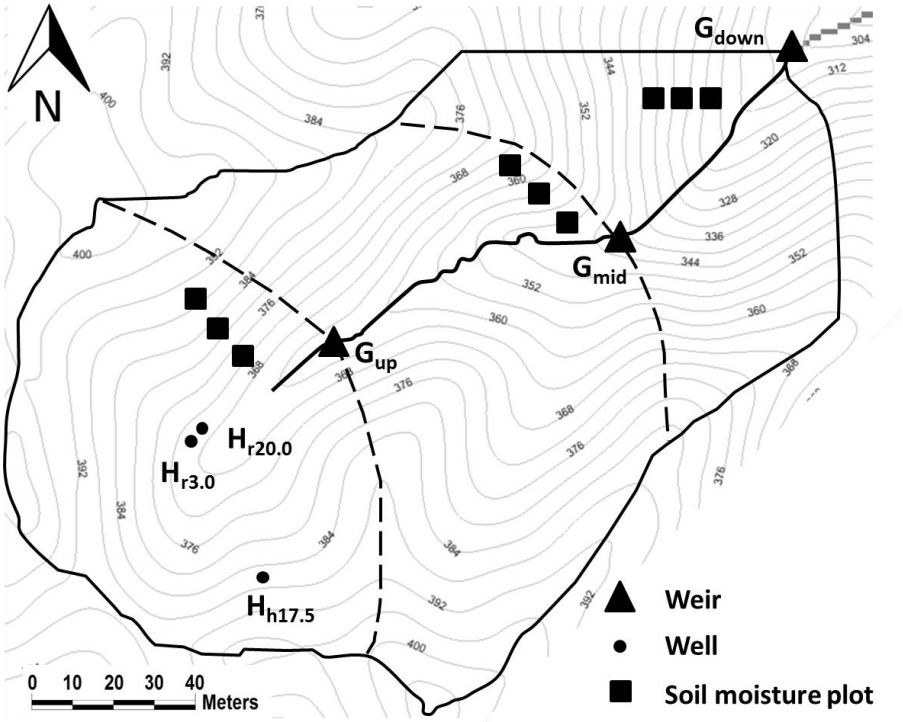

Fig. 3.1 Map of the study site in the Yayama Experimental Catchment (YEC) G_{up}, G_{mid} and G_{down} are the gauges; $H_{r3.0}$, $H_{r20.0}$, $H_{h17.5}$ are the groundwater wells. The dashed lines are for sub-catchment division. Contour interval is 4 m.

Groundwater level was monitored on the hillslope and in the riparian zone. A hillslope well ($H_{h17.5}$) was located upslope and installed to a depth of 17.5 m from the surface (Figure 3.1). Two wells of different depths were installed at the same location in the riparian zone to observe the vertical head gradient (VHG). A deep riparian well ($H_{r20.0}$) was installed to a depth of 20 m, with a screen present from 4 to 20 m. A shallow riparian well ($H_{r3.0}$) was installed to a depth of 3 m, with a screen present from 1 to 3 m. Elevation and horizontal distance between the ground locations of $H_{h17.5}$ and

H_{r20} were 15.2 and 36.6 m, respectively. Water level fluctuation in each well was recorded with a Hobo U20 water level data logger (Onset Company, Bourne, MA, USA) at 10-min intervals. Manual measurements of groundwater levels in each well were conducted twice per month to check sensor readings. The VHG between $H_{r20.0}$ and $H_{r3.0}$ was calculated by

$$VHG = \Delta h_1 / l_1 , \tag{3.1}$$

where Δh_1 is the head difference between $H_{r20.0}$ and $H_{r3.0}$ and l_1 is the horizontal distance between them.

The lateral head gradient (LHG) between $H_{h17.5}$ and $H_{r3.0}$ was calculated by

$$LHG = \Delta h_2 / l_2, \tag{3.2}$$

where Δh_2 is the head difference between $H_{h17.5}$ and $H_{r3.0}$ and l_2 is the horizontal distance between them.

Soil moisture was continuously monitored at three transects located on the hillslope at upstream, midtream and downstream. Each transect contains three soil moisture stations at toeslope, midslope and upslope (Figure 3.1, Figure 3.2). Each sampling station contained three soil moisture sensors at depths of 10 cm, 30 cm, and 50 cm (upstream and midstream transect: CS616, Campbell Scientific Inc., UT, USA; downstream transect: EC-5, Decagon Devices Inc., WA, USA) which collected data at 1-h intervals. The soil moisture was calibrated using the soil samples excavated from 3 soil pits on the hillslope where the soil moisture plot is located. The antecedent soil moisture index (ASI) (Haga et al., 2005) was calculated for each storm event as initial storage of the surface soil layer in the catchment, based on the volumetric water content at the measurement points:

$$ASI = \theta \times D, \tag{3.3}$$

where θ is the volumetric average soil water content (m^3/m^3) at depth of 0.1 m, 0.3 m and 0.5 m and D is the installation depth (0.5 m).

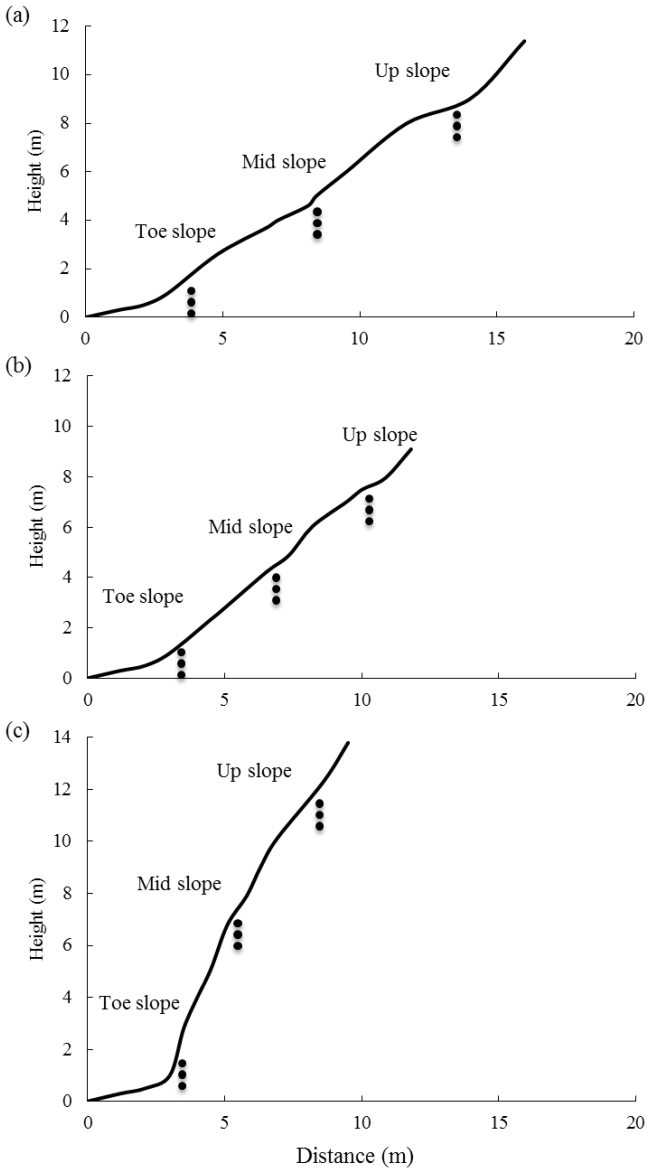

Fig. 3.2 Locations for soil moisture nests at (a) upstream, (b) midstream, (c) downstream. Each black dot represents a soil moisture sensor.

3.3 Results and discussion

3.3.1 Thinning effect on spatio-temporal streamflow generation

3.3.1.1 Thinning effect on water yield pattern

The annual precipitation in YEC during the two-year monitoring period was similar, comprising 2341 mm in 2011, and 2322 mm in 2013. At the nearby Uchino weather

station, the annual precipitation during this two-year monitoring period also was similar, being 2397 mm in 2011 and 2480 mm in 2013. For the years before the monitoring periods, the annual precipitation had similar values of 2632 mm in 2010 and 2547 in 2012. The mean annual precipitation from 1981 to 2011 at the nearby Uchino weather station was 2098 mm (± 387 mm). These data show that the study period covered relatively wet years in the region. The similarity in precipitation during the monitoring period and the years before enables us to compare the streamflow generation before and after thinning.

We divided the year 2013 into two periods based on the hyeto-hydrograph as we did for the year 2011. The dry period was January through late June when the water yield was low and relatively stable and early-September through December when the water yield slowly declined. The wet period was from the first major event recorded in June 19th through the rainy season to the end of typhoon season in early September, when the water yield increased due to the concentrated rainfall, which was longer than the wet period in 2011 from late May to mid-July.

We investigated the seasonal water yield pattern the same way as before thinning by comparing the water yield at G_{down}, G_{mid}, and G_{up}. During the baseflow time before the wet period, the water yield ranked in the order of G_{down}, G_{up}, and G_{mid} (Figure 3.3, Figure 3.4). However, values were similar among the three stations: all < 0.1 mm/h. During the baseflow time of the wet period, the water yield increased at each gauge site, and differences of water yield among the three gauges widened. Large differences in water yield between G_{mid} and the other gauges persisted for the remainder of the year. Water yield at G_{up} showed a slower increase than G_{down} at the beginning of the wet period but surpassed that of G_{down} in August (Figure 3.3, Figure 3.4). After the wet period, the difference in water yield between these gauges decreased, G_{up} had smaller values than G_{down} for the recession in September. G_{up} maintained larger values than G_{down} through the baeflow time from October to December (Figure 3.3, Figure 3.4). The seasonal trend of water yield pattern was consistent before and after thinning (Figure 2.3, Figure 3.4).

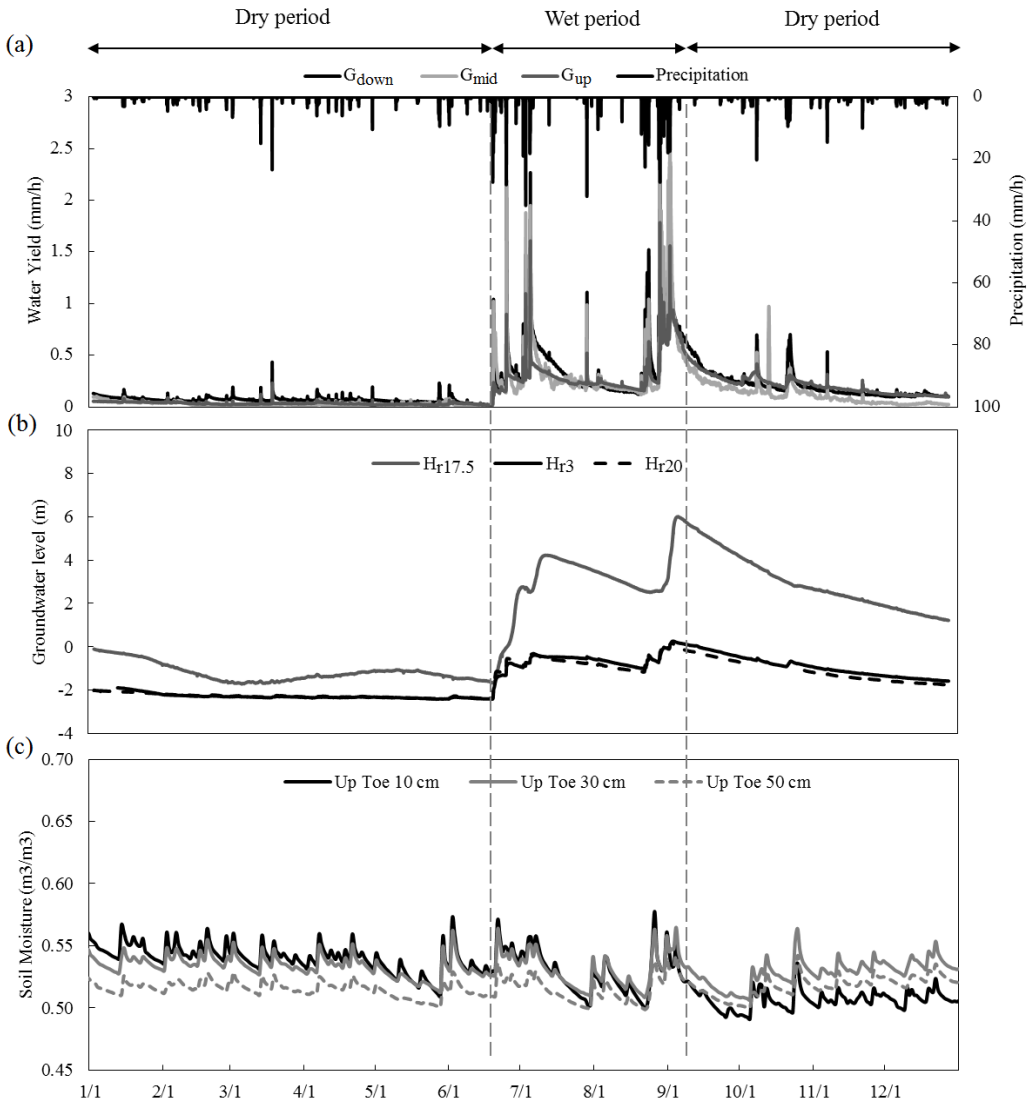

Fig. 3.3 (a) hydrograph, (b) groundwater, (c) upstream toe slope soil moisture in 2013. See the rest of the soil moisture data in the appendix. The vertical dashed lines are for season division. Zero point for the y-scale in groundwater represents the ground elevation of the riparian well.

3.3.1.2 Changes of baseflow generation after thinning

To examine the change in streamflow generation during baseflow after thinning, we investigated the groundwater contribution during baseflow. The hillslope groundwater showed similar trend after thinning compared to the year before thinning (Figure 2.2, Figure 3.3).

The hillslope groundwater table showed a steady decline from January, reaching the lowest level at late-June. Hillslope groundwater level rose as the rainy season began,

and peaked in September during the typhoon season (Figure 3.3). After the peak, the level gradually declined the rest of the year. The hillslope groundwater table remained within the weathered bedrock layer for the entire study period.

Riparian groundwater level also showed a similar trend after thinning compared to the year before thinning (Figure 3.3b). Riparian groundwater levels were stable from January through May and began to increase from a rain event on June 19th that produced 224 mm of precipitation. The riparian groundwater levels increased with each large rain event, peaking in September. During the rainy season, the stream expanded upstream to the area where $H_{r20.0}$ and $H_{r3.0}$ were located. Those levels declined gradually the remainder of the year. During the wet period, the riparian groundwater table could rise above the weathered bedrock layer into the soil. The riparian groundwater level declined gradually after wet period (Figure 3.3b).

To investigate the contribution of hillslope groundwater and riparian groundwater to baseflow, we examined the pattern of LHG and VHG the same way as we did before thinning. Same as in 2011, the LHG showed positive values throughout the year except for the event on June 20th in 2013. The VHG showed negative values from end of January to early July and for events during typhoon season in 2013, while due to less typhoon season precipitation, the negative values only appeared from early January to early July in 2011. The positive VHG value was from early July in the wet period till the end of year except typhoon weather in 2013, while it was from early July till the end of year in 2011 (Figure 3.3). The LHG and VHG show similar trend and coincide with the water yield pattern change before and after thinning (Figure 3.3).

After thinning, the VHG had positive values in 7/9—8/24 and 9/4—12/31. These two periods covered the baseflow period that upstream was higher than downstream. During the high baseflow time, hillslope contribution changed the streamflow recession magnitude. Delayed return flow contributes to storm during baseflow time after large rain events (Kosugi et al., 2006). After thinning, the seasonality of water yield pattern remained the same as before thinning. The thinning didn't change the dominant streamflow generation during baseflow in YEC. The porous weathered bedrock in YEC indicates long flow paths with groundwater dominant streamflow generation. YEC showed delayed and prolonged response to precipitation, which resulted in gradual

increase of baseflow during wet period and long recession after wet period. After thinning the increased throughfall during events (Matsuda, unpublished).

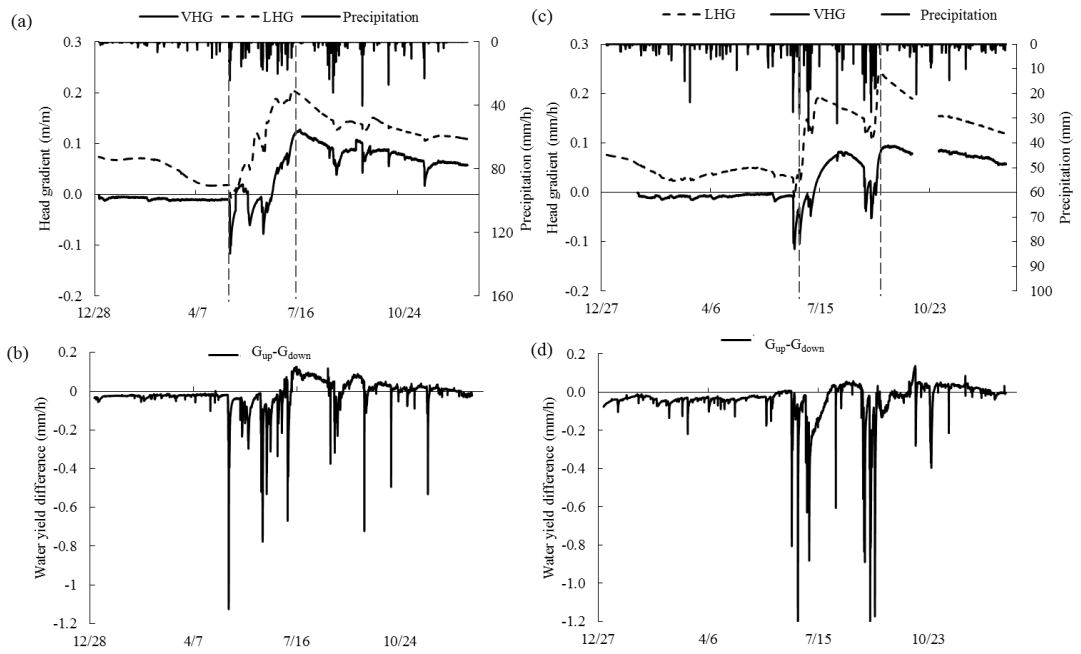

Fig. 3.4 Vertical hydraulic gradient (VHG) between $H_{r20.0}$ and $H_{r3.0}$ in (a) 2011 and (c) 2013, positive values mean riparian groundwater upwelling, and negative values mean riparian groundwater downwelling; lateral hydraulic gradient (LHG) between $H_{h17.5}$ and $H_{r3.0}$, positive value means hillslope groundwater contributing to riparian groundwater, negative values mean riparian groundwater contributing to hillslope groundwater; Water yield difference between G_{up} and G_{down} in (b) 2011 and (d) 2013, positive values mean $G_{up} > G_{down}$, negative values mean $G_{up} < G_{down}$.

3.3.1.3 Changes of stormflow generation after thinning

Hillslope soil moisture has been used as an indicator of hillslope-stream connectivity and throughflow (Burke and Kasahara 2011; Moore et al., 2011; Penna et al., 2011; Fu et al., 2013). In the present study, we compared hillslope soil moisture to streamflow and hillslope groundwater level to explain water movement during stormflow in the YEC the same way as before thinning.

The relationship between soil moisture and hillslope groundwater table was examined. We defined the discharge condition as when the hillslope groundwater level decreases continuously despite rainfall events (Figure 3.5a). The recharge condition was defined as groundwater level increase with rainfall events (Figure 3.5b). Hillslope

recharge and discharge condition before and after thinning were shown in Figure 3.6. The events with decrease of hillslope groundwater level during and after the event, suggesting that hillslope groundwater maintained a discharge trend because the precipitation amount was too small to influence the groundwater level (Figure 3.6, close circle). Conversely, the events with an increasing hillslope groundwater level with decreasing soil moisture, indicating recharge of hillslope groundwater level (Figure 3.6, open circle). Similar to before thinning, the recharge of groundwater mainly happened during wet period after thinning.

The relationship between soil moisture and water yield from the closest gauging station was examined. For most events in dry period, water yield increased and peaked before the hillslope soil moisture (Figure 3.5a). Water yield versus soil moisture shows clockwise hysteresis, which indicates no generation of subsurface flow (Sun et al., 2016). For the most events in wet period, water yield reacted more slowly than soil moisture, and peaked after the hillslope soil moisture peak (Figure 3.5b). For these events, water yield versus soil moisture shows counter-clockwise hysteresis, which indicates generation of subsurface flow (Sun et al., 2016). The hysteresis relationship between hillslope soil moisture and water yield showed that the subsurface flow was generated mainly in wet period both before and after thinning (Figure 2.5, Figure 3.7).

After thinning the seasonal patterns of soil moisture to water yield and soil moisture to groundwater remained similar (Figures 3.6 and 3.7), which indicated the appearance of hillslope groundwater recharge and subsurface flow during stormflow in the wet period. For most events in dry period, water yield increased and peaked before the hillslope soil moisture, suggesting that the hillslope contribution to stormflow was small. Water yield plotted versus soil moisture shows clockwise hysteresis. For the most events in wet period, water yield reacted more slowly than soil moisture, and peaked after the hillslope soil moisture peak, indicating a potential hillslope contribution to stormflow. For these events, the plot of water yield versus soil moisture shows counter-clockwise hysteresis. Subsurface flow may transfer pre-event soil water and dominate peak flow in steep headwater catchment (Bazemore et al, 1992). Thinning didn’t change the dominant stormflow response in YEC. The increased event water after thinning was buffered by the longer flow path.

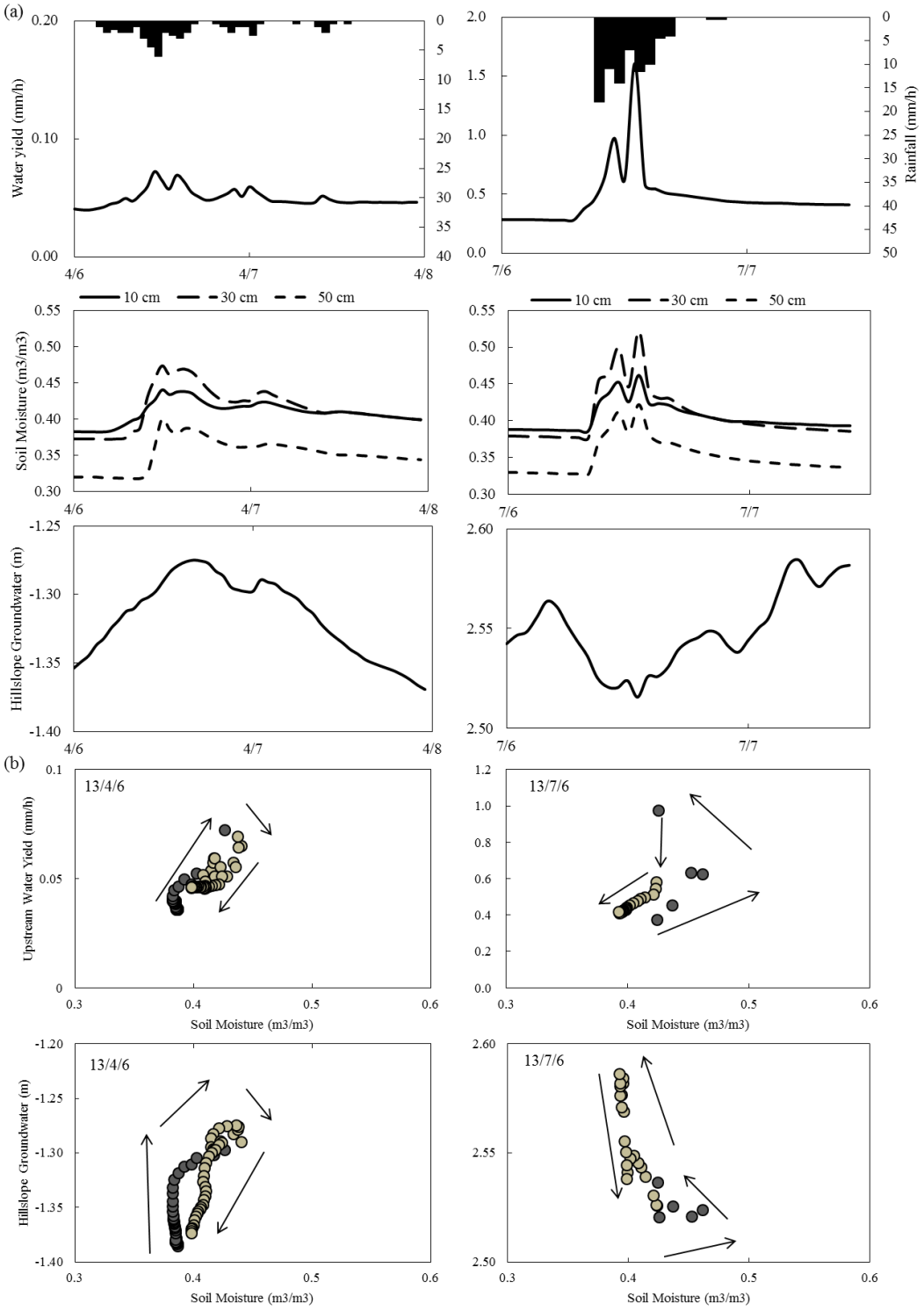

Fig. 3.5 a. Hydrograph and soil moisture and hillslope groundwater level during two events in 2013; b. 10 cm soil moisture plotted with upstream water yield for two events. Black dots represent the rising limb; light brown dots represent the falling limb.

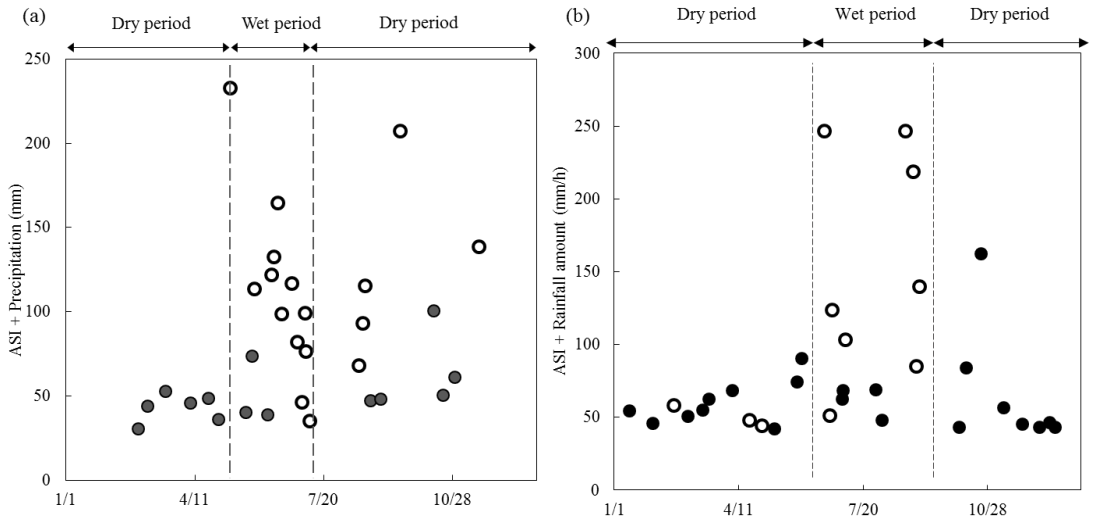

Fig 3.6 Temporal evolution of rainfall + ASI for the study year. a. 2011; b. 2013. Closed circles represent hillslope groundwater discharge conditions, open circles represent hillslope groundwater recharge conditions. The vertical dashed lines are for season division.

3.3.1.4 Effects of thinning on streamflow generation

Thinning of 50% in tree number has potential to change streamflow generation in headwater catchment. In YEC, the dominant streamflow generation didn't change after thinning. The groundwater dominant catchment underlain by porous weathered granite bedrock has high water storage, and allows long water flow path with long residence time (Sun et al., 2017). After thinning, the increased throughfall was stored in hillslope and released gradually through the year, which maintained the spatial water yield pattern. During events, the subsurface flow can contribute during rainy season and typhoon weather.

Even removal of 50% trees showed no changes in the dominant streamflow generation in a headwater catchment underlain by porous weathered granite, which indicated the water characteristics of weathered granite bedrock in storing water and buffering thinning effect. Longer monitoring period is desired for potential delayed changes after thinning in the catchment.

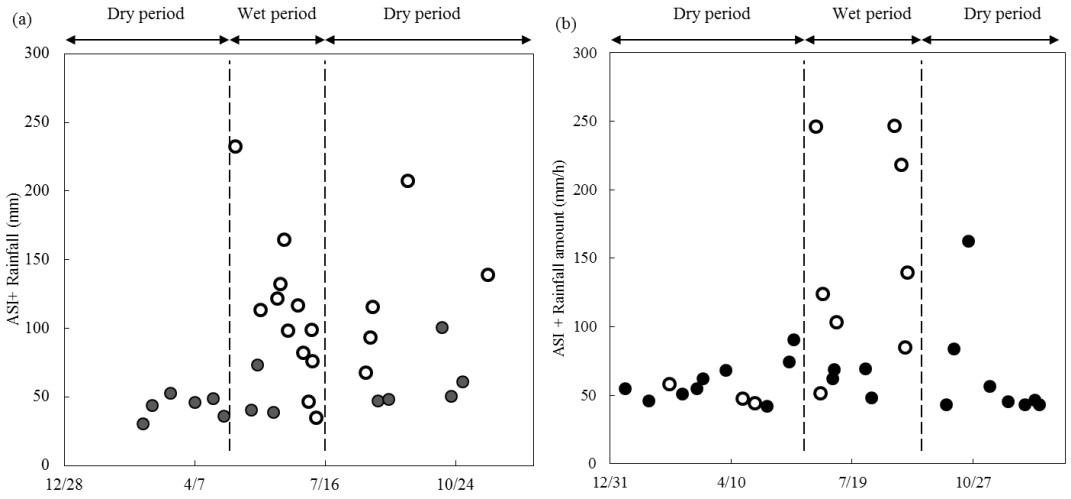

Fig 3.7 Temporal evolution of rainfall + ASI for the study year. a. 2011; b. 2013. Open circles represent clockwise hysteresis relationship between soil moisture and water yield; Closed circles represent counter-clockwise hysteresis relationship between soil moisture and water yield; the vertical dashed lines are for season division.

3.3.2 Hillslope contribution spatio-temporal variability

3.3.2.1 Hillslope contribution to baseflow

To further understand the riparian groundwater contribution to baseflow, we investigated the relationship between deep riparian groundwater and water yield in upstream and downstream. During the dry 1 period, deep riparian groundwater showed positive linear relationship with water yield in upstream, midstream and downstream (Figure 3.8). During the wet period and the dry 2 period, all the gauging stations exhibited similar linear relationship with deep riparian groundwater. At each gauging station, two positive linear relationships were found between deep riparian groundwater and the water yield for wet period and dry 2 period. The linear relationships with larger slope were days after rain events from July 8 to July 25 in 2013 (Figure 3.8).

Two positive linear relationships were found between deep riparian groundwater and the water yield for wet period and dry 2 period, which indicate extra water source contribution from hillslope rather than deep riparian groundwater. After large rain events, the whole catchment exhibited sustained hillslope groundwater contribution during the recession period, which caused steeper recession compared to other recession period in wet period and dry 2 period. During large rain events, the porous weathered

bedrock in YEC allows water to infiltrate deep into the hillslope and contribute to the stream days after the events. Similar hillslope contribution has been found in other gentle catchments, where different groundwater dynamics in riparian and hillslope caused the catchment to exhibit different recession behaviors (McGlynn et al., 2004; Penna et al., 2011). In steep catchment with relatively large hillslope water storage, the hillslope groundwater dynamics can also influence the recession behavior throughout the catchment.

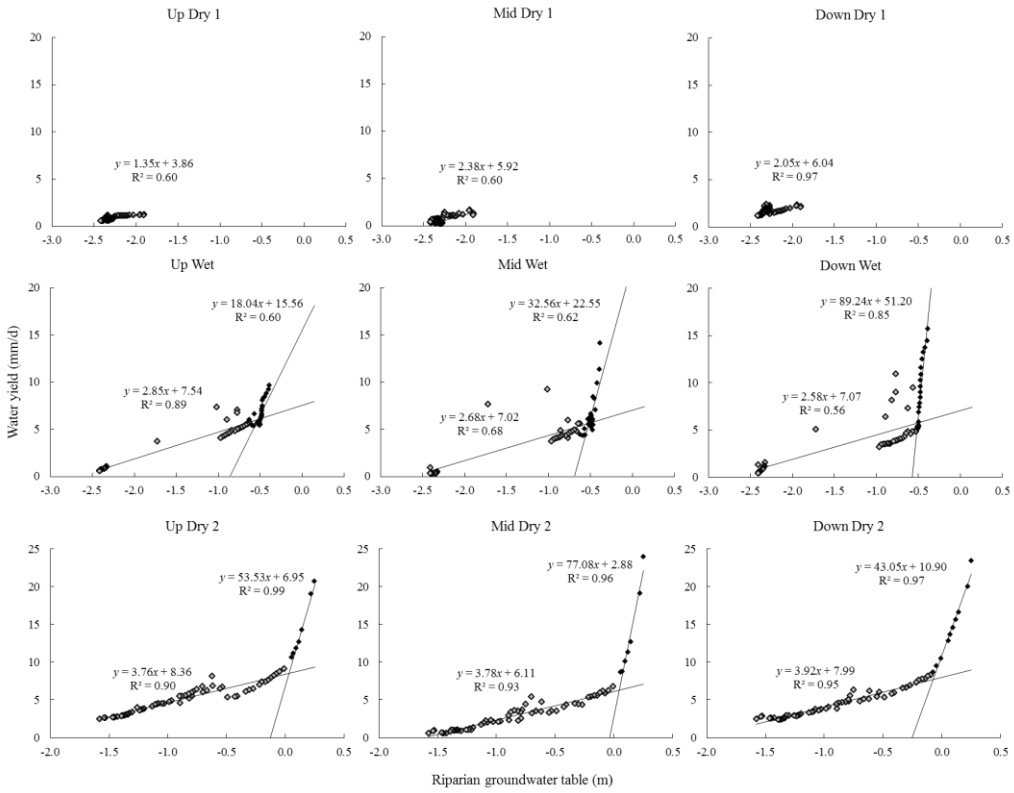

Fig 3.8 Relationship between deep riparian groundwater table and water yield at each gauge in each period during non-rainy days. Dry 1 indicates first half of dry period, Dry 2 indicates the second half of dry period. Grey symbol indicates weak reaction of water yield to riparian groundwater; Black symbol indicates strong reaction of water yield to riparian groundwater.

3.3.2.2 Hillslope contribution to stormflow

To further understand the spatial variation of hillslope subsurface flow, we examined soil moisture and water yield at upstream, midstream and downstream. Soil moisture in YEC exhibited flashy response to rainfall. A typical event with anti-clockwise hysteresis relationship between soil moisture and water yield on September 3rd with a

rainfall amount of 117 mm showed the quick and unified response of the same depth of soil moisture responded to rainfall peak (Figure 3.9). The differences in soil moisture were not prominent for the same depth in each transect.

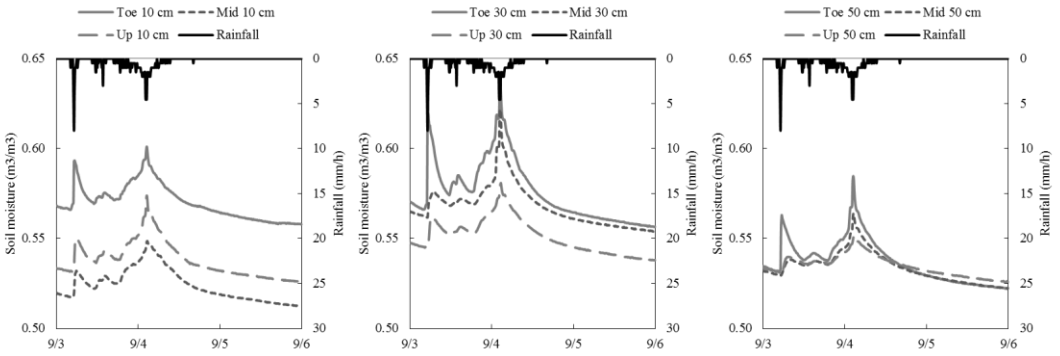

Fig 3.9 Same depth of soil moisture at different nests of upstream, midstream and downstream during a typical event on September 3rd with a rainfall amount of 117 mm.

The hysteresis relationship between hillslope soil moisture and water yield showed seasonality and spatial difference (Figure 3.10). During the dry period, when examining the hysteresis results from lowest point of all soil moisture transects, most events had a clockwise hysteresis relationship in upstream and midstream. For downstream, nine out of eighteen events exhibited counter-clockwise hysteresis (Figure 3.10). All gauging station showed counter-clockwise hysteresis during the event on October 23. During the wet period, seven out of fourteen events had counter-clockwise hysteresis for all the gauging stations, which all have over 80 mm rainfall amount (Figure 3.10).

For events with rainfall amount less than 100 mm, subsurface flow doesn't generate at upstream and midstream (Figure 3.10). Subsurface flow can generate at downstream, mainly for mid-sized events in dry period and dry-down period. Direct topographic control on streamflow generation is stronger in steep portion of a catchment where relatively gravitational influences on hydraulic gradients cause water to be transferred to stream quicker. The hillslope gradient in the upstream portion was 0.7. The steeper slopes within this flatter terrain appear to have a greater coverage of freely draining soils, which increase sub-surface flow (Tetzlaff et al., 2009).

For events with rainfall amount over 100 mm, subsurface flow generate at upstream, midstream and downstream (Figure 3.10). Studies carried out in gentle large catchments have reported gradual shrinking and expansion of connected area in hillslope (Jencso et

al., 2009; Jencso and McGlynn, 2011; Penna et al., 2011; Payn et al., 2012). In YEC, the steep hillslope showed shrinking and expansion of connected area under large rain events. However this behavior is flashier and more unified compared the gentle large catchments.

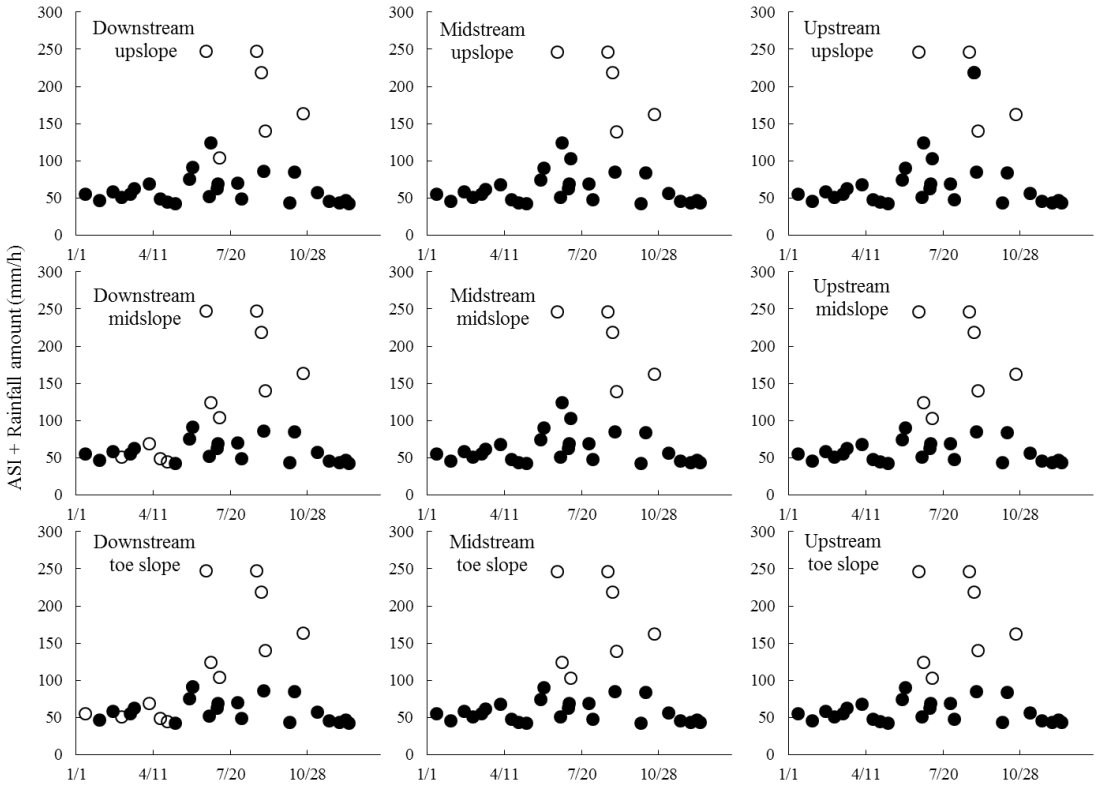

Fig 3.10 Temporal evolution of rainfall + ASI for the study year. Closed circles represent clockwise hysteresis relationship between soil moisture and water yield; Open circles represent counter-clockwise hysteresis relationship between soil moisture and water yield.

3.5 Conclusion

The spatio-temporal variation of streamflow generation processes after thinning in YEC were examined by comparing water yield pattern, groundwater table and spatial soil moisture dynamics. During baseflow, the relationship between deep riparian groundwater and water yield showed that downstream exhibited hillslope contribution from the steep hillslope in downstream area following rain events. During rain events, the hysteresis relationship between soil moisture and nearest gauging point showed that the hillslope subsurface flow contributed to runoff during heavy rain. The steep

hillslope showed flashy and unified shrinking and expansion of connected area under large rain events. The results showed even thinning of 50% in a headwater catchment underlain by porous granite bedrock didn’t change the dominant streamflow generation mechanism.

3.6 Summary

Streamflow generation can potentially be effected by thinning. However, thinning effect on spatial variations of streamflow generation processes in steep headwaters have not been well studied. In this chapter, we examined the spatio-temporal variation of streamflow generation processes after thinning in a steep 2.98-ha headwater catchment by comparing water yield pattern, groundwater level and soil moisture. Spatial water yield patter remained the same seasonality after thinning which was also controlled by deep groundwater upwelling at upstream. During rain events, the hysteresis relationship between soil moisture and nearest gauging point showed that the hillslope subsurface flow, same as before thinning, contributed to runoff during heavy rainy season and typhoon weather. The results of this chapter showed even thinning of 50% in a headwater catchment underlain by porous granite bedrock didn’t change the dominant streamflow generation mechanism.

Chapter 4

Effects of thinning on flow peaks in a forested headwater catchment

4.1 Introduction

In Japan, about 68% of the land surface is covered by forests on steep mountains (National Astronomical Observatory). Coniferous plantations, consisting largely of Japanese cypress and cedar, account for approximately 40% of this forested area (National Astronomical Observatory). It has been suggested that the decline in forest management over the past 30 years, linked to a recession-beleaguered forestry industry, has led to an increase in flood risk and soil erosion (Japan Forestry Agency; Onda 2010). Because of the sparse understory vegetation beneath a dense canopy in abandoned plantations, soil erosion and overland flow on hillslopes can easily occur (Sidle et al., 2007; Nanko et al., 2008; Gomi et al., 2010; Miura et al., 2010). As the area of abandoned or non-managed plantation forest increases, thinning to increase tree growth (Lesch et al., 1997) has emerged as a forest management tool to prevent environmental problems, such as erosion and floods (Onda 2010). After thinning, improved light conditions under the forest canopy can increase the growth of understory vegetation (Yanai et al., 1998). This growth can improve forest floor conditions by altering infiltration capacities and potential for shallow flow pathways (Grace et al., 2006).

Various studies have been undertaken to examine the effects of forest thinning on event flow (Bosch and Hewlett, 1992; Hornbeck et al., 1993; Stednick 1996; André assian 2004). However, their findings regarding changes in event flow characteristics have been inconsistent (Wright et al., 1990; Ruprecht et al., 1991; Grace et al., 2003; Rahman et al., 2005; Dung et al., 2012a; Choi et al., 2013).

Some studies have shown that forest thinning increases event peak flow (Wright et al., 1990; Ruprecht et al., 1991; Grace et al., 2003). For example, after selective thinning of 67% of the timber volume, the event peak flow of small storms was increased by 111% in a 424-ha catchment, with gentle slopes covered by redwood (*Sequoia sempervirens* (D. Don) Endl.) and Douglas fir (*Pseudotsuga menziesii* (Mirb.) Franco), located in Northwestern California, USA, under a Mediterranean climate (Wright et al., 1990). Likewise, random thinning of 84% (74% of basal area) increased event peak flows by 50% in an 80-ha catchment covered by jarrah (E. *marginata* Don ex Smith) and marri (E. *calophylla* Lindl.) in southwestern Western Australia, under a

climate having high winter rainfall, and hot dry summers (Ruprecht et al., 1991). Selective thinning of 70% trees (69% basal area) increased peak flow rates by 40% in a 60-ha catchment covered by 15-year-old loblolly pine (*Pinus taeda* L.) in North Carolina, USA, under a maritime temperate climate (Grace et al., 2003). In contrast, other studies have observed no changes in event peak flow after thinning (Rahman et al., 2005; Dung et al., 2012a; Choi et al., 2013). Thinning of 6% of the timber volume resulted in the event peak flow being unchanged in a 27.4-ha steep catchment covered with Japanese cedar (*Cryptomeria japonica*), Japanese cypress (*Chamaecyparis obtusa*), red pine (*Pinus densiflora*), and oak (*Quercus* spp.) in Kochi Prefecture, Japan, under a warm to temperate rainy climate (Rahman et al., 2005). Catchments that underwent thinning operations with high thinning percentages also showed no changes to their event peak flow (Dung et al., 2012a; Choi et al., 2013). For example, thinning of 58.3% (43.2% of basal area) in a 0.35-ha steep headwater catchment, covered by Japanese cypress (*Chamaecyparis obtusa*) in Mie Prefecture, Japan, under a moist temperate climate (0.70–1.00 m/m), did not affect event peak flow (Dung et al., 2012a). After 8.9–75.1% thinning of the basal area, no changes in event peak flow were detected in six catchments having gentle slopes (0.02–0.26 m/m), covered mainly by loblolly pine (*Pinus taeda* L.), with a lesser component of mixed hardwoods, in Mississippi, USA, under a humid subtropical climate (Choi et al., 2013).

The event peak response time, which is calculated as the time between the rainfall peak and event highest flow peak, has been reported to decrease after thinning (Wright et al., 1990, Ziemer, 1981). After logging and road construction, shorter event peak response times with steeper falling limbs were found; this is despite no changes in event peak flow in two catchments with areas of 424 ha and 473 ha (Sendek, 1985). In the six headwater catchments, where no event peak flow changes were observed after thinning of 8.9–75.1% of the basal area, the event peak response times were shortened in three catchments, associated with intense disturbance of the forest floor; whereas no changes in the event peak response times were observed in the other three catchments, associated with minimum disturbance of the forest floor (Choi et al., 2013).

Previous studies on the effect of thinning on rainfall-runoff processes have tended to examine only the characteristics of event peak flow, which is the highest peak of any

one event (Wright et al., 1990; Ruprecht et al., 1991; Grace et al., 2003; Rahman et al., 2005; Dung et al., 2012a; Choi et al., 2013). However, headwater catchments generally generate multiple flow peaks, directly responding to rainfall even during a single event; while down-stream larger catchments do not (McGlynn et al., 2004; Davies and Beven, 2015). Therefore, investigating all the flow peaks in headwater catchments is important to understanding changes in rainfall-runoff processes after thinning. This information provides deeper insights to the considerable effects of rainfall on sediment transport (Warburon 2010), nutrient transport (Alexander et al., 2007), and stream morphology (Beschta and Platts, 1986).

In this study, 50% of the trees in a steep headwater catchment, covered with Japanese cypress and cedar were thinned. Our objective was to examine the effects of thinning in a cypress and cedar tree plantation on rainfall-runoff characteristics. We hypothesized that the event peak flow and flow peaks would not be altered after thinning of 50% of the trees in this tree plantation. We undertook a single-catchment study and compared rainfall-runoff characteristics for similar rainfall periods in the year prior to and after the thinning exercise.

4.2 Site description

The Yayama Experimental Catchment (YEC) study site is a 2.98-ha headwater catchment. It is located in Fukuoka Prefecture (33°31’N, 130°39’E) on the island of Kyushu, Japan (Figure 4.1). The elevation of the catchment ranges from 305 to 406 m. The entire catchment is underlain by granite and its topography comprises steep slopes and narrow valley floors. The channel is incised in a section, where the channel gradient is steep; the mean hillslope gradient is 0.81 m/m, and the mean stream gradient is 0.37 m/m. According to a field survey by a drilling company (Abansu Corp.), the deeply weathered granite bedrock has a thickness of 13.7 m in the riparian area and 17.5 m on the hillslope. The riparian groundwater table is 2.5 m below the valley floor during the driest period and reaches ground level during the rainy season. The hillslope groundwater table measured at an upslope location is higher than the riparian groundwater table; it is 15 m below ground level during the driest period and reaches to 7 m below ground level during the rainy season. Four distinct soil layers within the

catchment are recognized, based on Dixfield–Marlow–Brayton general soil associations. The soil has a thickness of 70–100 cm, with high porosity (65%), and a high saturated hydraulic conductivity of 3.24 mm/min (Abansu Corp.; Takahashi, unpublished data).

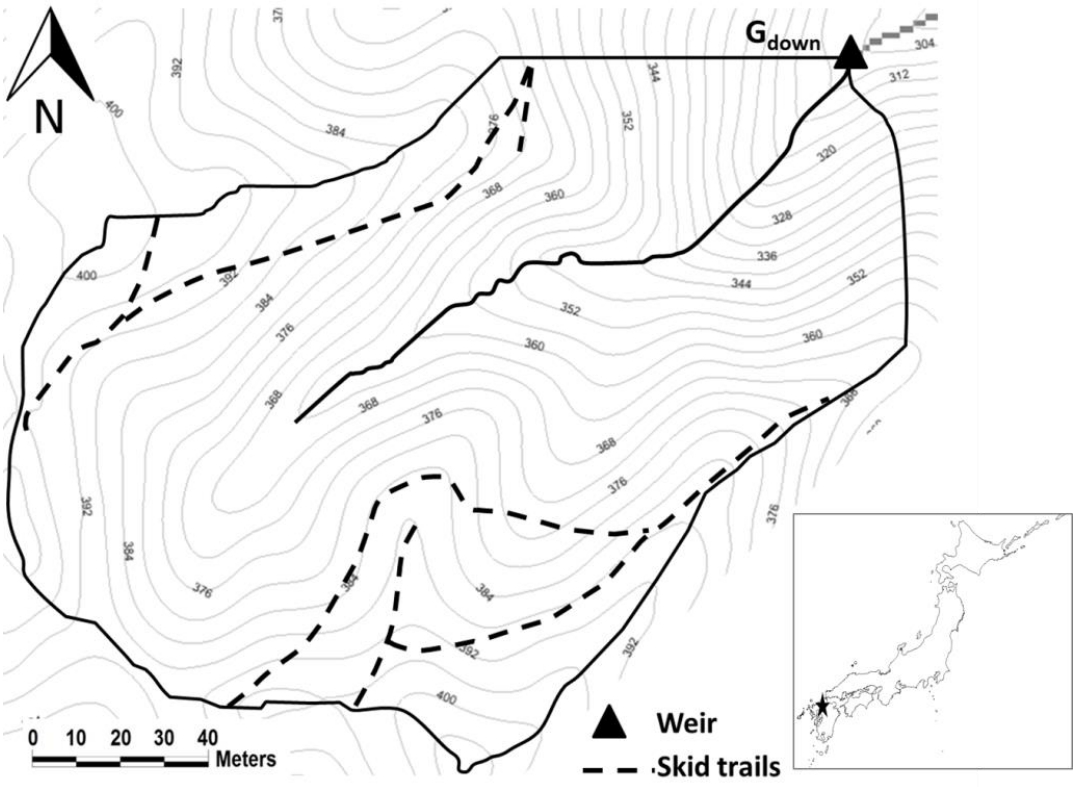

Fig 4.1 Map of the study site in the Yayama Experimental Catchment (YEC).

The average annual rainfall for the area is 2084 mm (1981–2010), based on rainfall data obtained from the nearby Uchino weather station (33°32’N, 130°38’E; 80 m a.s.l.), maintained by the Ministry of Land, Infrastructure, Transport, and Tourism. Precipitation falls occasionally as snow in January and February, and melts in early February. The rainy season is from mid-June to early July. Typhoon season is from mid-August to early September. Japanese cypress (*Chamaecyparis obtusa* Sieb. et Zucc.) and Japanese cedar (*Cryptomeria japonica* D. Don), planted in 1969, covered the catchment with a density of 1324 trees/ha and accounted for 67% and 33% of the entire stock before thinning in 2012, respectively (Tateishi et al., 2015).

4.3 Material and Methods

4.3.1 Field measurements

A single-catchment study was undertaken at the YEC from January 2011 to December 2013. Data from 2011 were used for the pre-thinning analysis, while those from 2013 were used for the post-thinning analysis. About 50% of the trees in the YEC were qualitatively thinned using chainsaws and removed during January–March 2012. The flow data for the rainy season of 2012 were not recorded because of equipment failure. Therefore, data for 2012 were not included in this study.

Rainfall was collected at a weather station located about 185 m southeast of the catchment, at an elevation of 390 m. A 0.5-mm tipping bucket rain gauge (TK-1; Takeda Keiki, Tokyo, Japan) was used, with data collected at 10-min intervals. An inter-storm period of at least 6 h without rain was used to identify rainfall events. Furthermore, only events with rainfall amounts of ≥5 mm were selected for analysis.

A stream gauging station (G_{down}), consisting of a V-notch weir and a Parshall flume, was installed at the outlet of the catchment (Figure 4.1). The V-notch gauge was used to monitor low flow, while the Parshall flume monitored high flow. The stage height was monitored at 10-min intervals in the V-notch weir and at 5-min intervals in the Parshall flume, using WT-HR water level loggers (TruTrack, Christchurch, New Zealand). Visual stage height readings and direct measurement of discharge were taken weekly during the wet season from June to July and bi-monthly during the reminder of the year to check and correct the stage-discharge relationship.

4.3.2 Flow separation

The quick flow component of the streamflow was separated using the digital filter method, proposed by Eckhardt (Eckhardt, 2005). The maximum baseflow index (BFImax) in the digital filter was estimated using the backwards filtering method, proposed by Collischonn and Fan (Collischonn and Fan, 2013). The quick flow was terminated, when the calculated baseflow equaled the actual flow. This method considers the geological characteristics of the catchment in the calculations, and it has

been successfully applied in several studies in which hydrograph separation has been performed (Gonzales et al., 2009; Lim et al., 2010). An event was defined as the beginning of rainfall to the end of its quick flow period, or the beginning of next rainfall event, when the quick flow was ongoing.

4.3.3 Definition of event flow and flow peaks

The parameters of the event flow in this study were defined as follows. The event peak flow was the highest flow in a single event (Figure 4.2a, A). The event peak response time was calculated as the time between the rainfall peak and the event highest flow peak (Figure 4.2a, B). Event water yield and event quick flow were calculated as the integration under the flood event hydrograph.

The parameters of flow peak in this study were defined as follows. Flow peaks were defined as all the peaks for a single event (Figure 4.2b, a_i). The flow peak response time was calculated as the time between the rainfall peak and the corresponding flow peak (Figure 4.2b, b_i). The initial flow was defined as the flow at the beginning of the rise in the hydrograph for the corresponding flow peak (Figure 4.2b, c_i). To exclude the effect of the rainfall prior to this rise in the hydrograph, we calculated the flow rise from the initial flow to the corresponding flow peak (Figure 4.2b, d_i). We also calculated the flow drop from the flow peak to the end of the falling limb, which coincides with the next initial flow, when succeeding flow peak exists (Figure 4.2b, e_i). Accumulated rainfall was calculated as the sum of the rainfall for the period between the initial flow and the corresponding flow peak (Figure 4.2b, f_i). Accumulated quick flow was calculated as the sum of the quick flow for the period between the initial flow and the subsequent initial flow or the end of the falling limb (Figure 4.2b, shaded area).

4.3.4 Statistical analysis

Streamflow data do not usually follow the probability distributions on which many statistical methods are based. Therefore, application of nonparametric statistical methods is required. Here, the Mann–Whitney U test (u-test), which is sensitive to differences in the mean (H_0: mean ranks of runoff values of two classes in the same group are similar), was applied (Wilks, 2011). Analysis of covariance (ANCOVA) was

applied to assess the effect of thinning on event peak flow, event quick flow, event water yield, flow peak, accumulated quick flow, flow rise, and flow drop parameters.

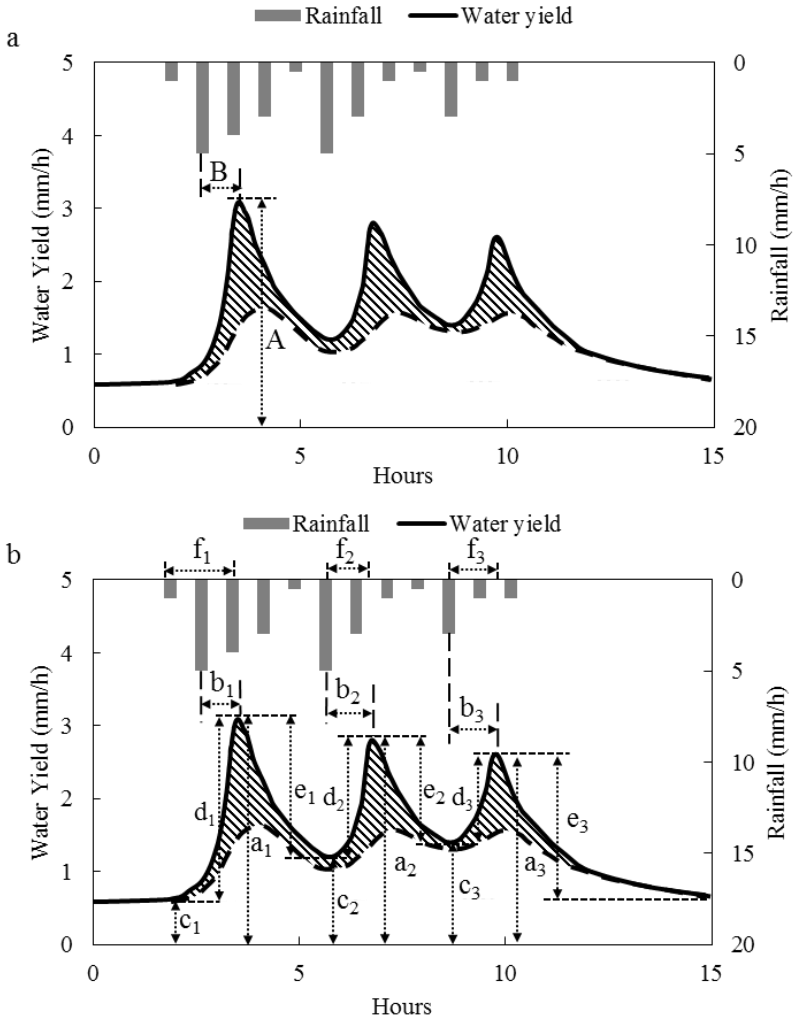

Fig. 4.2 Schematics diagram of an event with 3 flow peaks showing (a) event flow characteristics: A. event peak flow (mm/h), B. event peak response time (h), and shaded area which indicates event quick flow; and (b) flow peak characteristics: a_i. flow peak (mm/h), b_i. flow peak response time (h), c_i. initial flow (mm/h), d_i. flow rise (mm/h), e_i. flow drop (mm/h), f_i. accumulated rainfall (mm), and shaded area which indicates accumulated quick flow for each peak.

4.4 Results and discussion

The annual precipitation in YEC during the two-year monitoring period was similar, comprising 2341 mm in 2011, and 2322 mm in 2013. At the nearby Uchino weather station, the annual precipitation during this two-year monitoring period also was similar,

being 2397 mm in 2011 and 2480 mm in 2013. For the years before the monitoring periods, the annual precipitation had similar values of 2632 mm in 2010 and 2547 in 2012. The mean annual precipitation from 1981 to 2011 at the nearby Uchino weather station was 2098 mm (± 387 mm). These data show that the study period covered relatively wet years in the region. The similarity in precipitation during the monitoring period and the years before enables us to perform event flow analysis. There were 67 and 64 events with rainfall amounts of ≥5 mm, before and after thinning, respectively, which were concentrated between June and September (Figure 4.3). The sum of the event water yield was 608 mm before thinning in 2011, and 687 mm after thinning in 2013.

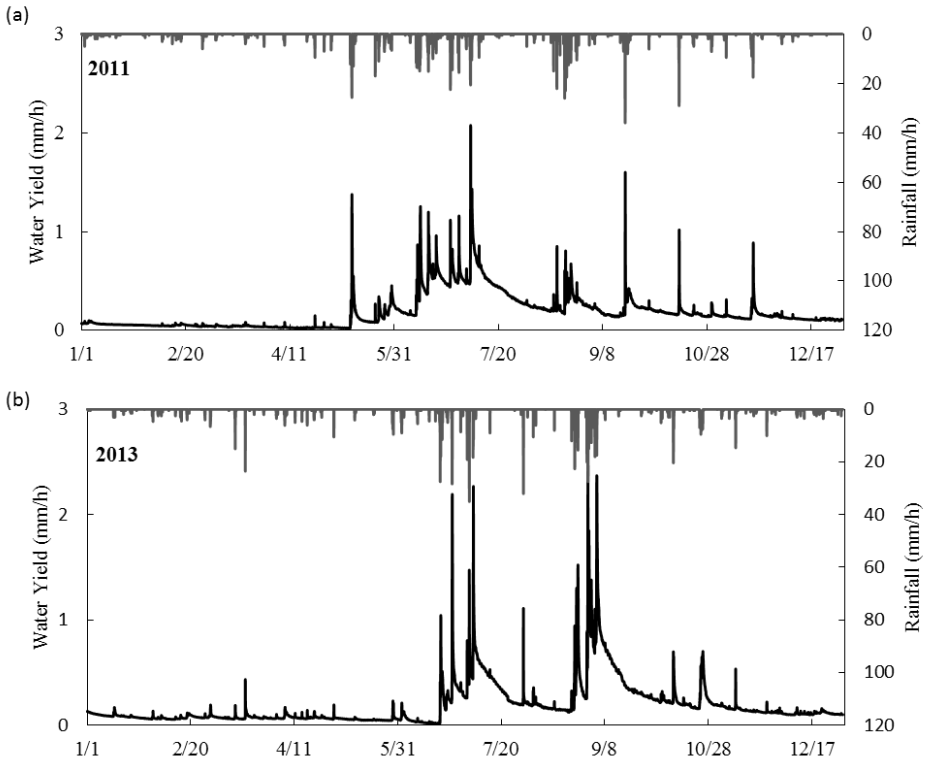

Fig 4.3 Hydrograph and hyetograph in the YEC in (a) 2011 and (b) 2013.

4.4.1 Changes in event flow after thinning

The rainfall-runoff characteristics before and after thinning were firstly compared at event flow basis. The changes in event flow after thinning were examined based on the relationships between rainfall amount and event peak flow, event quick flow and event water yield (Figure 4.4). There were no differences in the relationships between rainfall

amount and event peak flow (ANCOVA: p = 0.45), event quick flow (ANCOVA: p = 0.14) and event water yield (ANCOVA: p = 0.93), for events documented before and after thinning.

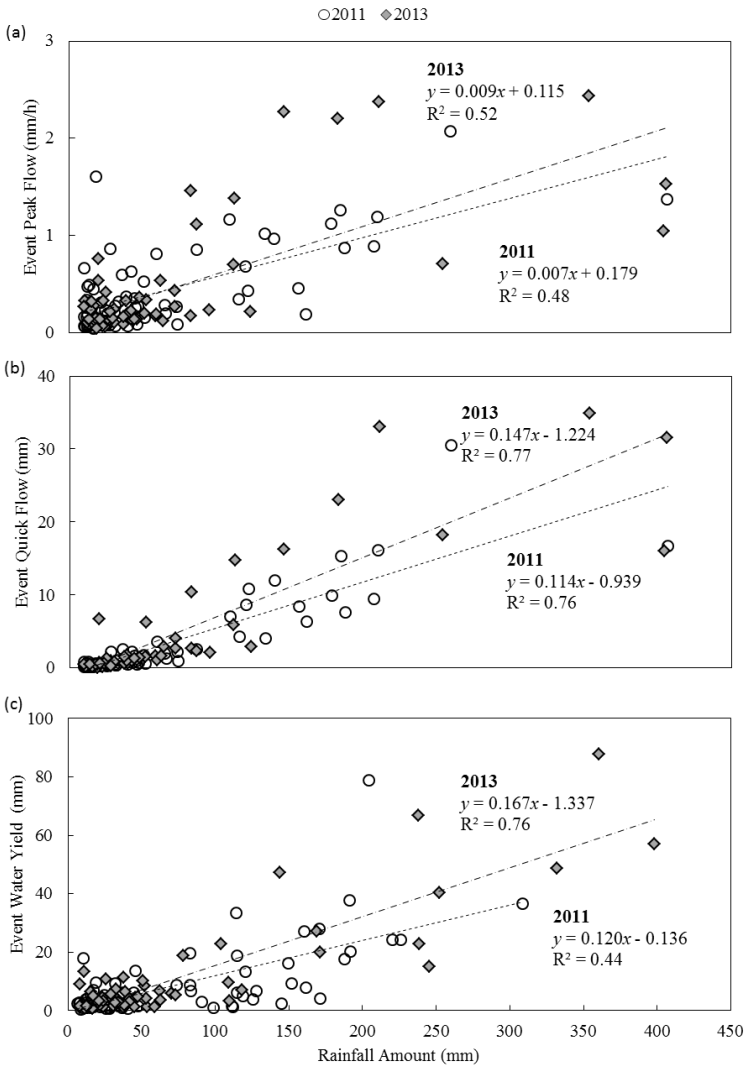

Fig 4.4 Rainfall amount in relation to (a) event peak flow; (b) event quick flow; (c) event water yield for all the events in 2011 and 2013.

To explore the changes in event flow after thinning for similar rainfall event size, we categorized the events into four groups. We selected a rainfall amount of 30 mm and an average rainfall intensity of 2 mm/h as the criteria with which to divide the events, because 46% and 47% of events recorded before and after thinning had rainfall amount <30 mm and average rainfall intensity <2 mm/h (Figure 4.5). The event flow characteristics of each group are summarized in Table 4.1. The number of events within

each group was similar before and after thinning, which allowed us to examine changes in event flow (Table 4.1).

The event peak flow, the event quick flow, and the event water yield were all found to increase only for events with rainfall amount ≥30 mm and average rainfall intensity ≥ 2mm/h after thinning. However, as shown in the u-test in Table 4.1, no significant changes were found in the event peak flow, the event quick flow, or the event water yield for median values, before and after thinning in any group. The ANCOVA tests also showed no significant changes in the relationship between event peak flow, the event quick flow, and the event water yield with rainfall amount. Neither were significant changes found in the event peak response time (Table 4.1).

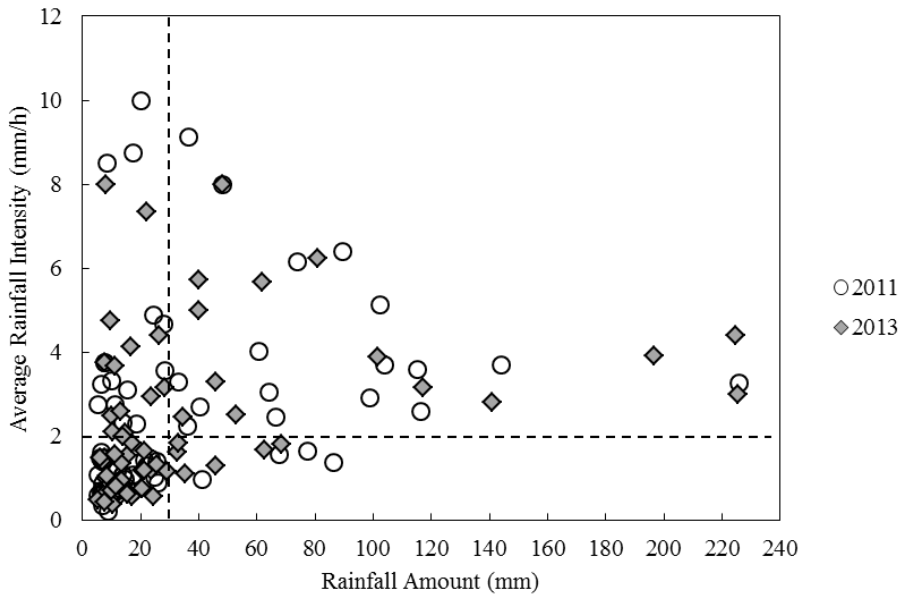

Fig 4.5 Scatter plot of rainfall amount (mm) and average rainfall intensity (mm/h) for all the events in 2011 and 2013.

No changes of rainfall-runoff characteristics during events were revealed after thinning of 50% in the YEC. For catchment with similar thinning percentage, Dung et al. (2012b) found thinning of 58.3% in a 0.35-ha steep headwater catchment (0.70–1.00 m/m) did not affect event peak flow. In catchments with thinning percentages lower than 50%, Rahman et al. (2005) and Choi et al. (2013) also reported no event peak flow changes after thinning. However, previous thinning studies only focused on event-based hydrographs. Only performing event flow analysis may omit important rainfall-runoff

Table 4.1 Summary of event flow characteristics in 2011 (Before) and 2013 (After), *p*-values are listed in the u-test and ANCOVA results section.

Rainfall amount (mm)		<30				≥30			
Ave. rainfall intensity (mm/h)		<2		≥2		<2		≥2	
Group number		1		2		3		4	
		2011	2013	2011	2013	2011	2013	2011	2013
Number of events		31	30	15	14	4	6	17	14
Event rainfall amount (mm)	Average	12.6	14.0	12.9	15.4	68.1	46.3	85.6	100.8
	Median	10.5	12.0	14.0	13.5	72.5	40.8	74.0	71.5
Event peak flow (mm/h)	Average	0.17	0.17	0.46	0.23	0.48	0.37	0.85	1.23
	Median	0.16	0.13	0.33	0.21	0.43	0.18	0.86	1.07
Event quick flow (mm)	Average	0.4	0.9	0.8	0.6	8.0	4.2	8.6	14.4
	Median	0.4	0.4	0.5	0.4	9.6	2.7	7.0	13.2
Event water yield (mm)	Average	4.0	4.6	4.9	3.4	21.7	12.3	18.9	30.5
	Median	2.1	3.1	3.8	1.7	22.8	7.2	13.3	22.8
Event peak response time (h)	Average	0.9	0.7	0.9	0.9	1	0.8	1.3	0.9
	Median	1	1	1	1	1	1	1	1
Event peak flow	u-test	0.19		0.59		0.26		0.47	
	ANCOVA test	0.76		0.19		0.51		0.18	
Event quick flow	u-test	0.28		0.59		0.77		0.15	
	ANCOVA test	0.14		0.44		0.87		0.11	
Event water yield	u-test	0.16		0.27		0.59		0.33	
	ANCOVA test	0.83		0.34		0.93		0.24	
Event peak response time	u-test	0.25		0.74		0.81		0.48	

changes after thinning, particularly the flow peaks other than event peak flow. Therefore, apart from the aforementioned traditional analysis of event flow, we proposed alternative analysis of flow peaks, taking all flow peaks during events into account, which provided a better linkage between rainfall and runoff characteristics.

4.4.2 Flow peaks changes after thinning

To augment our study, we analyzed all flow peaks for all the events. There were 194 flow peaks for the 67 events before thinning, among which 49 events had multiple flow peaks, covering 127 flow peaks that were not event peak flow. Similarly, there were 184 flow peaks for the 64 events after thinning, among which 43 events had multiple flow peaks, covering 120 flow peaks that were not event peak flow (Figure 4.6). The average duration of the flow peaks changed from 10.9 h before thinning to 11.6 h after thinning. The recession time, which is the time it takes for the flow peak to decrease by the calculated flow drop, changed from 7.6 h to 8.2 h.

The relationships of the accumulated rainfall with the flow peak, the accumulated quick flow, the flow rise, and the flow drop are illustrated in Figure 4.7. Our results indicate that the flow peak (ANCOVA: $p = 0.30$) did not show any significant increases with accumulated rainfall (Figure 4.7a). However, the flow rise (ANCOVA: $p = 0.01$), and the flow drop (ANCOVA: $p = 0.02$) showed significant increases with accumulated rainfall after thinning (Figure 4.7b, c). The accumulated quick flow (ANCOVA: $p = 0.03$) also showed significant increases with accumulated rainfall after thinning (Figure 4.7d).

In the YEC, the larger flow drop led to the lower initial flow of the subsequent peak, which resulted in no increase in the flow peak, despite the significant increase in flow rise after thinning (Figure 4.8). The larger flow rise and flow drop combined with the similar duration and magnitude of the flow peaks led to the larger accumulated quick flow after thinning (Figure 4.8).

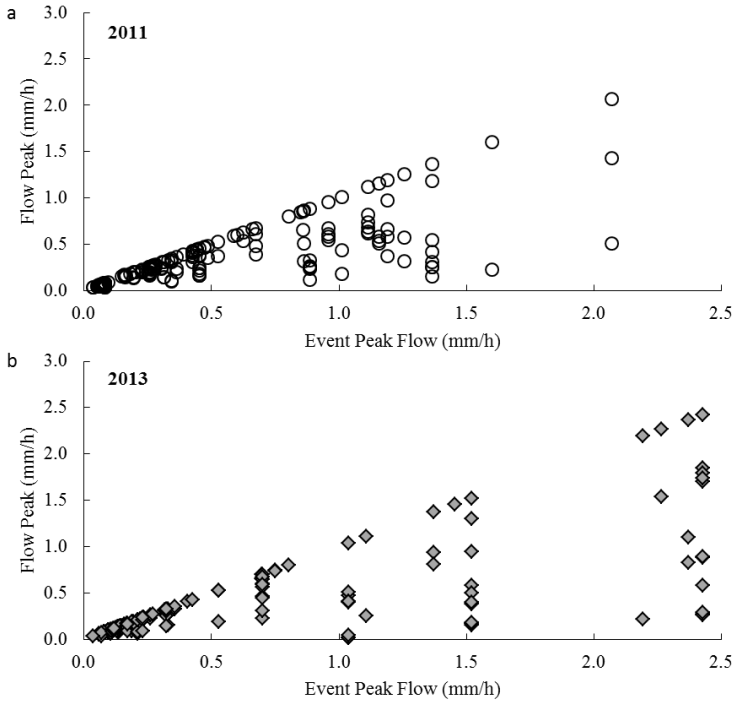

Fig. 4.6 Event peak flow in relation to flow peak (a) 2011; (b) 2013.

To investigate the effects of thinning on flow peaks in detail, we grouped each flow peak, based on the same criteria used in the event flow analysis, i.e., a rainfall amount of 30 mm, and an average rainfall intensity of 2 mm/h (Table 4.2, Figure 4.9). The number of flow peaks and accumulated rainfall for each group were similar before and after thinning (Table 4.2, Figure 4.9a).

In group 4, large increases were found for all averages and medians of flow peak, flow rise, flow drop, and accumulated quick flow (Table 4.2, Figure 4.9). In groups 1, 2 and 3, the average and median of each parameter changed, although changes were small (Figure 4.9). The average flow peak response time decreased in all groups. Flow peak, flow rise, flow drop, and accumulated quick flow in group 4 showed a significant increase. Accumulated quick flow in group 1 showed a significant increase. Flow peak in group 2 showed a significant decrease, although the sample size is small. Flow peak response time in groups 1 and 4 showed significant decreases after thinning (Table 4.2).

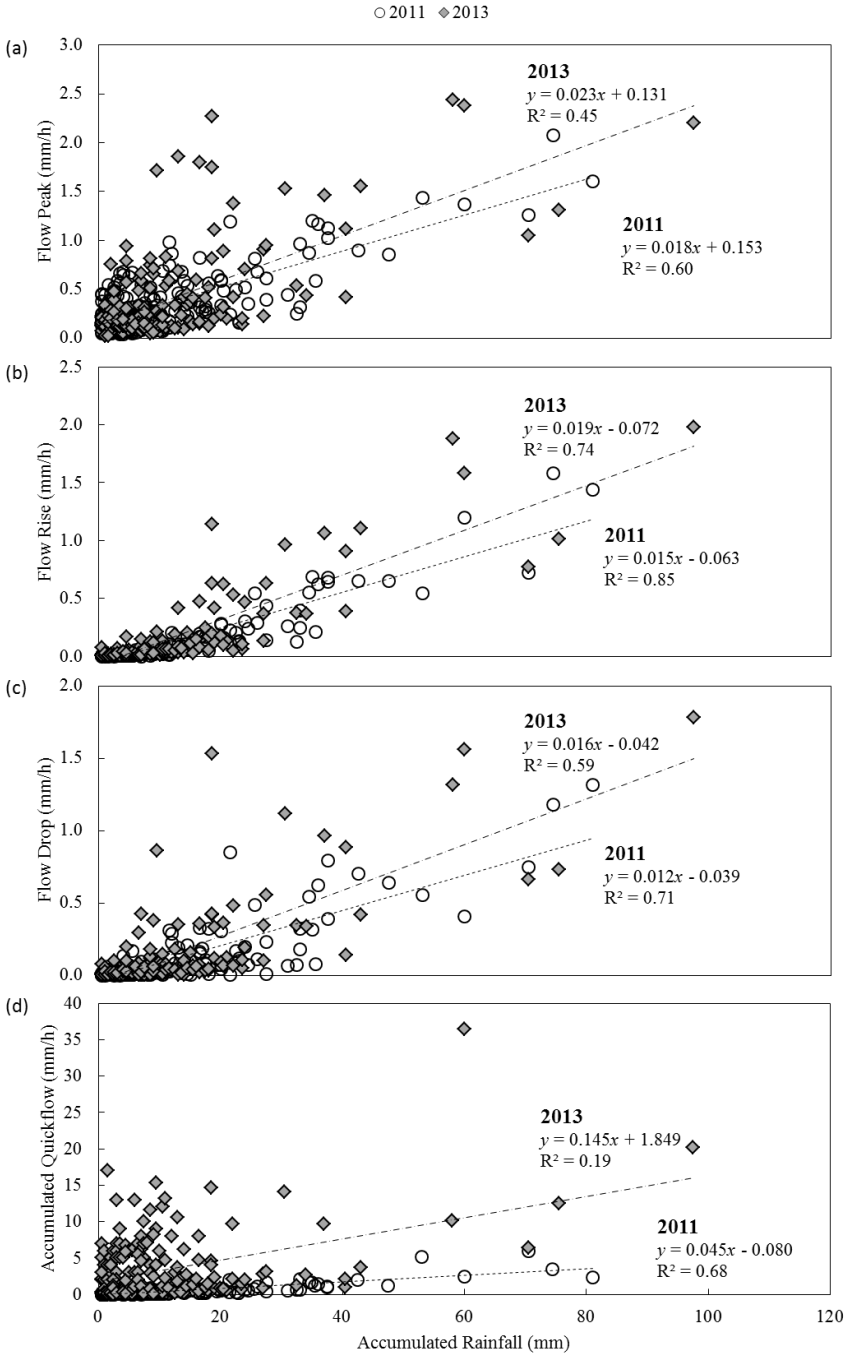

Fig. 4.7 Accumulated rainfall in relation to (a) flow peak; (b) flow rise; (c) flow drop; (d) accumulated quick flow for all the flow peaks in 2011 and 2013.

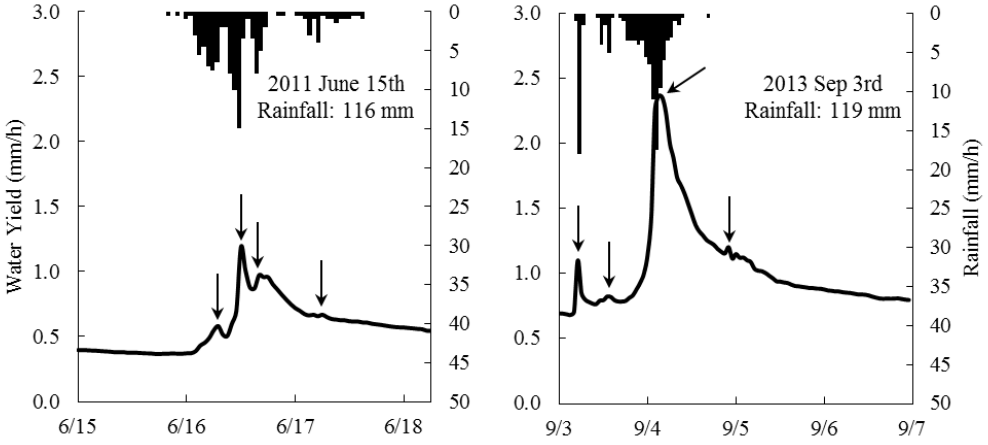

Fig. 4.8 Hydrographs for typical events selected in 2011 (left) and 2013 (right), arrows indicated the selection of flow peaks.

4.4.3 Comparisons of event flow and flow peaks

Although no changes in the event peak flow, event quick flow, and event peak response time were found before and after thinning in our event flow analysis, changes were revealed in the flow rise, flow drop, accumulated quick flow and flow peak response time after thinning using a flow peak analysis. The flow peaks show a more direct link between rainfall and runoff, and the changes observed in the characteristics of these flow peaks suggest that the rainfall-runoff characteristics changed after thinning. In particular, we found significant changes in flow peak characteristics of group 1 and group 4.

In group 1, the flow rise increased and the flow peak response time was shortened after thinning (Table 4.2, Figure 4.9). Although previous studies have not focused on a flow peak analysis, in event-based studies, relative interception loss (the ratio of interception to rainfall) would be high during events with small rainfall amount (Xiao et al., 2000; Ward, 2010). Leaf area index (LAI) was measured in a Japanese cypress plot and a Japanese cedar plot before and after thinning. During events having less than 10 mm accumulated rainfall in the YEC, the closed canopy before thinning (LAI = 3.80 $m^2 m^{-2}$ in the Japanese cypress plot and LAI = 3.50 $m^2 m^{-2}$ in the Japanese cedar plot) could intercept more rainwater than

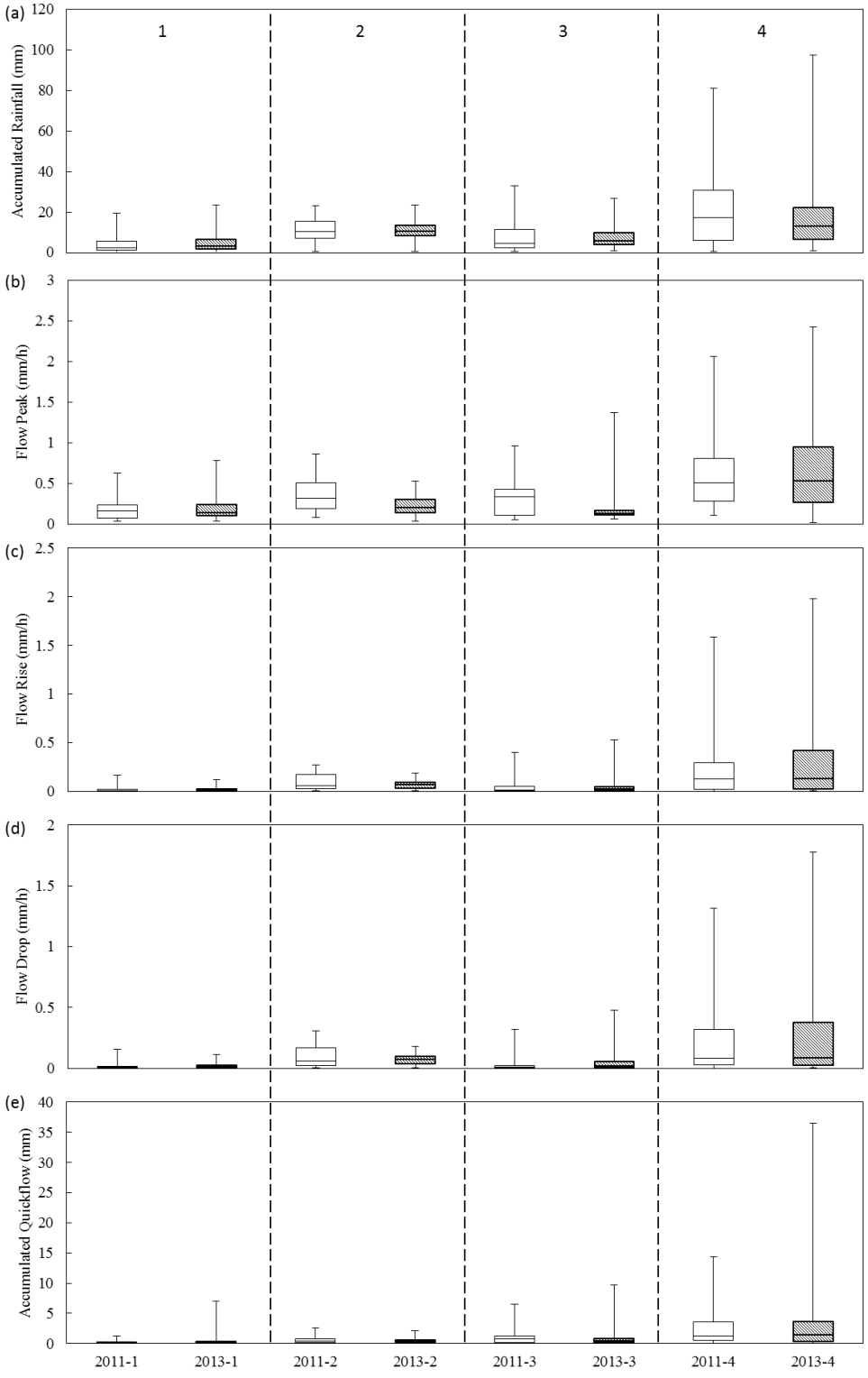

Fig. 4.9 Box plot of (a) accumulated rainfall; (b) flow peak; (c) flow rise; (d) flow drop; (e) accumulated quick flow for each group of flow peaks in 2011 (blank box) and 2013 (shaded box). The horizontal line within the box indicates the median, boundaries of the box indicate the 25^{th}- and 75^{th} -percentile, the whiskers indicate the highest and lowest values of the results and dashed lines are for group divisions.

Tab 4.2 Summary of flow peaks characteristics in 2011(Before) and 2013 (After), p-values are listed in the u-test and ANCOVA results section.

Rainfall amount (mm)		<30				≥30			
Ave. rainfall intensity (mm/h)		<2		≥2		<2		≥2	
Group number		1		2		3		4	
		2011	2013	2011	2013	2011	2013	2011	2013
Number of flow peaks		84	77	19	19	30	27	61	61
Accumulated rainfall (mm)	Average	4.1	4.5	11.1	10.7	7.9	8.2	20.9	18.9
	Median	2.5	3.0	10.5	10.5	4.8	5.5	17.5	13.0
Flow peak (mm/h)	Average	0.18	0.18	0.36	0.22	0.31	0.23	0.60	0.73
	Median	0.16	0.13	0.31	0.20	0.33	0.12	0.51	0.53
Flow rise (mm/h)	Average	0.02	0.02	0.09	0.07	0.04	0.05	0.25	0.33
	Median	0.01	0.01	0.06	0.07	0.01	0.02	0.12	0.13
Flow drop (mm/h)	Average	0.02	0.02	0.09	0.07	0.04	0.05	0.22	0.30
	Median	0.01	0.01	0.06	0.07	0.01	0.02	0.08	0.09
Accumulated quick flow (mm)	Average	0.15	0.41	0.72	0.56	1.23	1.09	2.47	3.70
	Median	0.09	0.17	0.40	0.31	0.74	0.48	1.29	1.48
Flow peak response time (h)	Average	0.9	0.6	0.8	0.7	0.6	0.5	1.0	0.4
	Median	1.0	0.0	1.0	1.0	0.0	0.0	1.0	0.0
Accumulated rainfall	u-test	0.67		0.95		0.51		0.35	
Flow peak	u-test	0.73		**0.04**		0.06		0.64	
	ANCOVA test	0.94		**0.02**		0.17		**0.02**	
Flow rise	u-test	**0.03**		0.66		**0.02**		0.65	
	ANCOVA test	0.79		0.21		0.77		**<0.01**	
Flow drop	u-test	**0.03**		0.95		0.51		0.72	
	ANCOVA test	0.34		0.34		0.48		**0.01**	
Accumulated	u-test	**<0.01**		0.68		0.30		0.68	

quick flow	ANCOVA test	**0.01**	0.49	0.68	**0.03**
Flow peak response time	u-test	**<0.01**	0.46	0.75	**<0.01**

the sparse canopy after thinning (LAI = 0.77 $m^2 m^{-2}$ in the Japanese cypress plot and LAI = 0.84 $m^2 m^{-2}$ in the Japanese cedar plot) (Tateishi et al., 2015). The increased through fall after thinning indicates that more water reaches the forest floor, and contributes to runoff, which may lead to a larger flow rise and a quicker catchment runoff response.

In group 4, the flow peaks exhibited a significant increase in flow peak, flow rise, flow drop and accumulated quick flow (Table 4.2, Figure 4.9). During intense rainfall after thinning, the rapid increase and decrease in flow indicates that the catchment exhibited more shallow flow paths. Based on event scale analysis, canopy interceptions were measured in the YEC and found to decrease from 23.1% to 22.4% in the Japanese cypress plot and from 27.2% to 21.5% in the Japanese cedar plot, after thinning (Matsuda, unpublished data). The decreased interception after thinning caused more throughfall. In the YEC, during large accumulated rainfall events, the saturated area extends to the hillslope, while the shallow groundwater in the riparian area reacts quickly to rainfall (Sun et al., 2016). The contribution of extra water from throughfall after thinning may allow shallow riparian groundwater to generate more throughflow, causing the rapid increase and decrease of flow observed at this site. In a small forested catchment in Western Australia, throughflow from perched shallow groundwater increased after thinning, which led to the increase in event peak flow (Ruprecht et al., 1991).

Previous studies examined the effect of thinning on rainfall-runoff processes using only event-based hydrographs; some studies showed no changes after thinning (Dung et al., 2012a; Dung et al., 2012b; Choi et al., 2013). This study also showed no changes after thinning, when event-based hydrographs were analyzed. However, we observed changes significant in flow peaks. Thus, thinning affected the rainfall-runoff processes in the YEC, suggesting the importance of considering all flow peaks, especially in

headwater catchments. Further investigation of the changes in flow peaks in studies dealing with the effects of thinning may reveal changes in rainfall-runoff processes that might not be detected in an event-based analysis. In future study, multi-year comparisons of flow peak characteristics should be carried out.

4.5 Conclusions

Thinning of tree numbers by 50% was performed in the YEC, a steep headwater catchment in Japan, covered with Japanese cypress and cedar planted in 1969. Changes in rainfall-runoff characteristics were examined in the year prior to and after thinning. Event based analysis did not reveal any significant changes after thinning. To capture the effects of thinning on rainfall-runoff characteristics more effectively, we examined all the flow peaks for all rainfall events. Increases in the accumulated quick flow, flow rise, flow drop were detected for these events. The flow drop during the falling limb of each flow peak increased, and led to a lower initial flow in the subsequent peak, which yielded no increase in the flow peaks. The changes in rainfall-runoff characteristics were significant during flow peaks in events with over 30 mm rainfall amount and over 2 mm/h average rainfall intensity. After thinning of the cypress and cedar tree plantation, the catchment exhibited more shallow flow paths during large rainfall events. These changes may induce higher flood risk and soil erosion during early post-thinning years. Further study, assessing the combined effects of understory vegetation and flow peak changes on flood risk and erosion problem needs to be carried out to evaluate these risks.

4.6 Summary

This chapter examined the changes in rainfall-runoff characteristics in the year prior to and after intensive thinning of 50% in number in a steep headwater catchment, covered with Japanese cedar and cypress planted in 1969 in western Japan. The magnitude of event peak flow, event quick flow, event water yield, and event response time did not change after thinning. Because 70% of rainfall events had multiple flow peaks, relationships between each flow peak and the rainfall just prior to that peak were also analyzed. The increases in accumulated quick flow, flow rise and flow drop were significant after thinning. The flow drop following each flow peak increased, and led to

a lower initial flow in subsequent peaks, resulting in no increase in peak size. The flow peaks in events with over 30 mm rainfall amount and over 2 mm/h average rainfall intensity showed significant increases in flow peak, flow rise, flow drop, and accumulated quick flow, which suggests that the catchment exhibited more shallow flow paths during large rainfall amounts after thinning. No changes were identified using event-based analysis, but changes in flow peaks were detected, which indicates the importance of examining all flow peaks, when investigating rainfall-runoff characteristics of headwater catchments.

Chapter 5

Summary and conclusion

This study was conducted to understand the spatio-temporal streamflow generation mechanisms and rainfall-runoff characteristics under thinning, artificial changing environment, in forested headwater catchment underlain by granite. This study showed several findings which are summarized as follows.

In Chapter 2, the results showed that the time when baseflow of the upstream section exceeded that of downstream coincided with the time when the riparian groundwater switched from downwelling to upwelling. This suggested that upwelling of the riparian groundwater increased considerably in the upstream section during the wet period, resulting a shift in the relative size of baseflow between the upstream and downstream sections. The timing of fluctuations among hillslope soil moisture, hillslope groundwater and streamflow revealed that the hillslope contributed to stormflow, but this contribution was limited to the wet period. Therefore, streamflow generation has strong spatial variations, even in small, steep headwater catchments.

In Chapter 3, the spatio-temporal variation of streamflow generation processes after thinning were examined by comparing water yield pattern, groundwater level and soil moisture. Spatial water yield patter remained the same seasonality after thinning which was also controlled by deep groundwater upwelling at upstream. During baseflow, the relationship between deep riparian groundwater and water yield showed that downstream exhibited hillslope contribution following large rain events. During rain events, the hysteresis relationship between soil moisture and nearest gauging point showed that the hillslope subsurface flow, same as before thinning, contributed to runoff during heavy rainy season and typhoon weather. The results of this chapter showed even thinning of 50% in a headwater catchment underlain by porous granite bedrock didn’t change the dominant streamflow generation mechanism.

In Chapter 4, the effects of thinning on rainfall-runoff characteristics was clarified. Because 70% of events had multiple flow peaks, and 65% of the flow peaks are not event peak flow, clarifying the flow peak characteristics is of great importance to understand rainfall-runoff characteristics. The results showed that the magnitude of event peak flow, event quick flow, event water yield and event response time did not change after thinning. The relationships between each flow peak and the rainfall just prior to that peak were also analyzed. The increase in accumulated quick flow, flow rise

and flow drop was significant after thinning. The flow drop during the falling limb of each flow peak increased and led to a lower initial flow in the subsequent peak resulting in no increase in peak size. The flow peak in events with over 30 mm rainfall amount and over 2 mm/h average rainfall intensity showed significant increase in flow peak, flow rise, flow drop, and accumulated quickflow which suggested that the catchment exhibited more shallow flow paths during large rainfall amounts after thinning.

As mentioned, this study clarified the spatio-temporal streamflow generation mechanisms and rainfall-runoff characteristics after thinning in forested headwater catchment underlain by granite. As a result, the following answers were obtained.

(1) Streamflow generation has strong spatial variations, even in small, steep headwater catchments. The streamflow generation in steep headwater catchment is closely related to hillslope groundwater and subsurface flow dynamics.

(2) Thinning of 50% in a headwater catchment underlain by porous granite bedrock didn't change the dominant spatio-temporal streamflow generation mechanism.

(3) Thinning of 50% trees in number didn't change the rainfall-runoff characteristics in a headwater catchment underlain by porous weathered granite bedrock. However, thinning may result in significant changes in flow peaks during large rainfall events in early post-thinning years.

Overall, the spatial variation of streamflow generation in small steep headwater catchments is closely related to hillslope groundwater and subsurface flow dynamics. Thinning of 50% trees in number didn't change the dominant spatio-temporal streamflow generation and the rainfall-runoff characteristics in a headwater catchment underlain by porous weathered granite bedrock. During early post-thinning years, however, the YEC exhibited significant changes in flow peaks during large rainfall events after thinning, which may induce flood risk and soil erosion. These results are valuable to understanding of catchment hydrologic models and forest management practices.

Appendix

Soil moisture for upstream, midstream and downstream nests

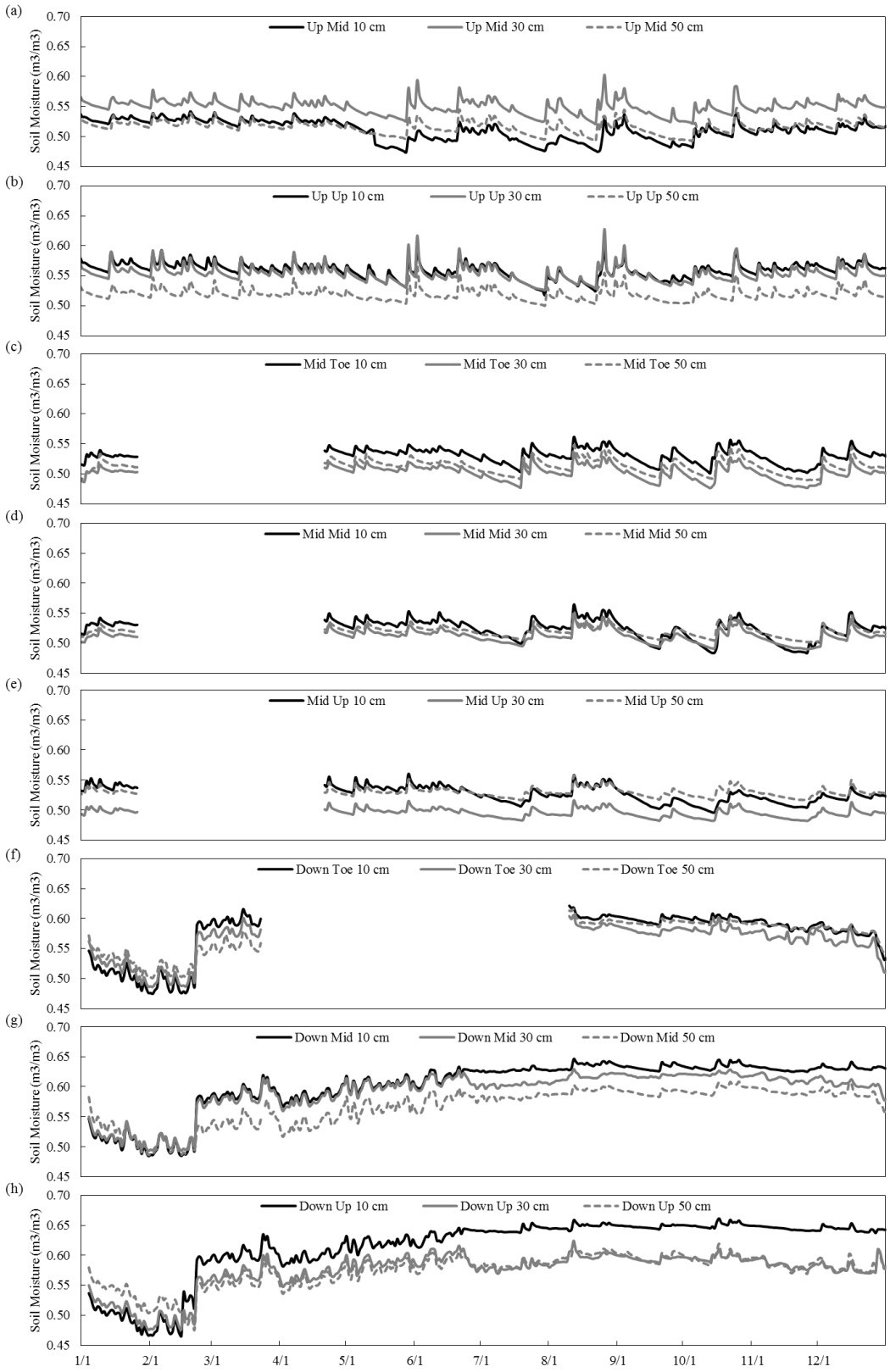

Fig. (a) upstream mid slope soil moisture; (b) upstream up slope soil moisture; (c) midstream toe slope soil moisture; (d) midstream mid slope soil moisture; (e) midstream up slope soil moisture; (f) downstream toe slope soil moisture; (g) downstream mid slope soil moisture; (h) downstream up slope soil moisture in 2013

Acknowledgement

During my studies at Kyushu University, I have received the assistance from many individuals and funding agencies. This dissertation would not have been possible without their help and support.

First, I would like to thank my supervisor, Professor Kyoichi Otsuki (Kyushu University), for the time, effort and outstanding support he devoted to my research, the innumerable skills and life lessons he taught me, and valuable comments during the writing of manuscript, submission process and the writing of this dissertation.

I also express my deep gratitude to Dr. Tamao Kasahara (Kyushu University) who is my advisor. She taught me how to become a field hydrologist and always urged me to think outside the box, which has been a major influence on my growth and success as a PhD candidate.

I appreciate Dr. Masaaki Chiwa (Kyushu University) for his kindly and helpful advices. I cannot get my degree without his comments and help.

I also appreciate the helpful suggestions during the seminars from the professors of the laboratory of forest ecosystem management (Takuo Hishi, Ayumi Katayama).

I am also grateful to all members of the laboratory of forest ecosystem management (Kyushu University) in the past and at the present. They (Yoshiyuki Miyazawa, Ryuji Ichihashi, Yoshinori Shinohara, Kenji Tsuruta, Jun'ichiro Ide, Makiko Tateishi, Fumiko Iwanaga, Yoshitoshi Uehara, Baolin Xue, Kenichi Shinozuka, Yang Xiang, Vansath Sisadeth, Sodouangdenh Somsanouk, Hiroki Matsuda, Seonghun Jeong) contributed much to my work through helpful discuss.

I would like to express my gratitude to the administrative and technical staffs of the research forest of Kyushu University.

With the help and support from so many people around me, I was able to finish this study and obtain the PhD degree. I thank all of you and am proud that I worked with you.

Financial support for this study was provided by the Core Research for Evolutional Science and Technology (CREST) project of the Japan Science and Technology Agency (JST) entitled “Development of innovative technologies for increasing catchment runoff and improving river environments by development of management practices for devastated forest plantations” and Fukuoka Prefecture Foundation for Headwater Forests. Fukuoka Prefecture Foundation for Headwater Forests and JSPS KAKENHI Grant (Adjustment of stand density control diagram for water resource conservation) Number 26292088.

Finally, I express my heartfelt thanks to my beloved family. Without their kindly encouragement and support, I cannot come to Kyushu University and finish my doctoral degree.

Bibliography

Abdul AS, Gillham RW. (1984) Laboratory studies of the effects of the capillary fringe on streamflow generation. Water Resource Research, 20(6), 691-698, DOI: 10.1029/WR020i006p00691

Alexander RB, Boyer EW, Smith RA, Schwarz GE, Moore RB. (2007) The role of headwater streams in downstream water quality. Journal of American Water Resource Association, 43(1), 41-59, http://doi.org/10.1111/j.1752-1688.2007.00005.x.

Anderson MG, Burt TP. (1978) Role of topography in controlling throughflow generation. Earth Surface Processes and Landforms, 3(4), 331-344.

Anderson SP, Dietrich WE, Montgomery DR, Torres R, Conrad ME, Loague K. (1997) Subsurface flow paths in a steep, unchanneled catchment. Water Resources Research 33(12), 2637-2653.

Andréassian V. (2004) Waters and forests: from historical controversy to scientific debate. Journal of Hydrology, 291, 1-27, http://doi.org/10.1016/j.jhydrol.2003.12.015.

Bachmair S, Weiler M, Troch PA. (2012) Intercomparing hillslope hydrological dynamics: Spatio-temporal variability and vegetation cover effects. Water Resources Research, 48, W05537.

Bari MA, Smith N, Ruprecht JK, Boyd BW. (1996) Changes in streamflow components following logging and regeneration in the southern forest of Western Australia. 10(3), 447-461, DOI: 10.1002/(SICI)1099-1085(199603)10:3<447::AID-HYP431>3.0.CO;2-1.

Barthold FK, Wu J, Vaché KB, Schneider K, Frede H-G, Breuer L. (2010) Identification of geographic runoff sources in a data sparse region: hydrological processes and the limitations of tracer-based approaches. Hydrological Processes, 24, 2313-2327.

Benda L, Hassan MA, Church M, May CL. (2005) Geomorphology of steepland headwaters: the transition from hillslope to channels. Journal of the American Water Resources Association, 41, 835-851.

Beschta RL, Platts WS. (1986) Morphological Features of Small Streams: Significance and Function. Journal of the American Water Resources Association, 22(3), 369-379, http://doi.org/10.1111/j.1752-1688.1986.tb01891.x.

Beven KJ, Kirkby MJ. (1979) A physically based, variable contributing area model of basin hydrology. Hydrological Sciences Journal, 24, 43-69.

Beven KJ. (2006) Streamflow generation processes. Wallingford: IAHS Press.

Bloomfield JP, Bricker SH, Newell AJ. (2011) Some relationships between lithology, basin form and hydrology: a case study from the Thames basin, UK. Hydrological Processes, 25, 2518-2530.

Bond BJ, Jones JA, Moore G, Phillips N, Post D, McDonnell JJ. (2002) The zone of vegetation influence on baseflow revealed by diet patterns of streamflow and vegetation water use in a headwater basin. Hydrological Processes, 16, 1671-1677.

Bosch JM, Hewlett JD. (1982) A review of catchment experiments to determine the effect of vegetation changes on water yield and evapo-transpiration. Journal of Hydrology, 55, 3-23, https://doi.org/10.1016/0022-1694(82)90117-2

Botter G, Peratoner F, Putti M, Zuliani A, Zonta R, Rinaldo A, Marani M. (2008) Observation and modeling of catchment-scale solute transport in the hydrologic response: A tracer study. Water Resources Research, 44, W05409.

Bronstert A, Niehoff D, Bürger G. (2002) Effects of climate and land-use change on storm runoff generation: present knowledge and modelling capabilities. Hydrological Processes, 16(2), 509-529. DOI: 10.1002/hyp.326.

Burke AR, Kasahara T. (2011) Subsurface lateral flow generation in aspen and conifer-dominated hillslopes of a first order catchment in northern Utah. Hydrological Processes, 25, 1407-1417.

Burt TP. (1992) The hydrology of headwater catchments. In: The Rivers Handbook, P. Calow and G.E. Petts (Editors). Blackwell, London, United Kingdom, pp. 3-28.

Burt TP, McDonnell JJ. (2015) Whither field hydrology? The need for discovery science and outrageous hydrological hypotheses, Water Resource Research, 51: 5919–5928, DOI:10.1002/2014WR016839.

Buttle JM, McDonald DJ. (2002) Coupled vertical and lateral preferential flow on a forested slope, Water Resource Research, 38(5), doi:10.1029/2001WR000773.

Chen L. Yuan Z, Shao H, Wang D, Mu X. (2014) Effects of thinning intensities on soil infiltration and water storage capacity in a Chinese pine-oak mixed forest. the Scientific World Journal. DOI: http://dx.doi.org/10.1155/2014/268157.

Choi B, Hatten JA, Dewey JC, Otsuki K, Cha D. (2013) Effect of timber harvesting on stormflow characteristics in headwater streams of managed, forested watersheds in the Upper Gulf Coastal Plain in Mississippi. Journal of the Faculty of Agriculture, Kyushu University, 58, 395-402.

Collischonn W, Fan FM. (2013) Defining parameters for Eckhardt's digital baseflow filter. Hydrological Processes , 27, 2614-2622, https://doi.org/10.1002/hyp.9391.

Davies JAC, Beven K. (2015) Hysteresis and scale in catchment storage, flow and transport. Hydrological Processes, 29, 3604-3615, http://doi.org/10.1002/hyp.10511.

Decagon Devices. (2006) Operator's manual for Models EC-20, EC-10, and EC-5. Version 2.2. Decagon Devices, Pullman, WA.

Dung BX, Gomi T, Miyata S, Sidle RC, Kosugi K, Onda Y. (2012a) Runoff responses to forest thinning at plot and catchment scales in a headwater catchment draining Japanese cypress forest. Journal of Hydrology, 444-445, 51-62, http://doi.org/10.1016/j.jhydrol.2012.03.040.

Dung BX, Gomi T, Miyata S, Sidle RC. (2012b) Peak flow responses and recession flow characteristics after thinning of Japanese cypress forest in a headwater catchment. Hydrological Research Letter, 6, 35–40, http://doi.org/10.3178/hrl.6.35.

Dunne T, Black RD. (1970) An Experimental Investigation of Runoff Production in Permeable Soils. Water Resources Research, 6, 478-490.

Dunne T, Black RD. (1970) Partial Area Contributions to Storm Runoff in a Small New England Watershed. Water Resources Research, 6, 1296-1311.

Eckhardt K. (2005) How to construct recursive digital filters for baseflow separation. Hydrological Processes, 19, 507-515, https://doi.org/10.1002/hyp.5675.

Freer J, McDonnell JJ, Beven KJ, Peters NE, Burns DA, Hooper RP, Aulenbach B, Kendall C (2002) The role of bedrock topography on subsurface storm flow. Water Resource Research, 38, 5-1-5-16.

Frisbee MD, Allan CJ, Thomasson MJ, Mackereth R. (2007) Hillslope hydrology and wetland response of two small zero-order boreal catchments on the Precambrian Shield. Hydrological Processes, 21, 2979-2997.

Fu CS, Chen JY, Jiang HB, Dong LY. (2013) Threshold behavior in a fissured granitic catchment in southern China: 1. Analysis of field monitoring results. Water Resources Research, 49, 2519-2535.

Gomi T, Sidle RC, Richardson JS. (2002) Understanding Processes and Downstream Linkages of Headwater. System Biosciences, 52 (10): 905-916. DOI:10.1641/0006-3568(2002)052[0905:UPADLO]2.0.CO;2.

Gomi T, Asano Y, Uchida T, Onda Y, Sidle RC, Miyata S, Kosugi K, Mizugaki S, Fukuyama T, Fukushima T. (2010) Evaluation of storm runoff pathways in steep nested catchments draining a Japanese cypress forest in central Japan: a geochemical approach. Hydrological Processes, 24, 550–566, http://dx.doi.org/10.1002/hyp.7550.

Gonzales AL, Nonner J, Heijkers J, Uhlenbrook S. (2009) Comparison of different base flow separation methods in a lowland catchment. Hydrology and Earth System Sciences, 13, 2055-2068, https://doi.org/10.5194/hess-13-2055-2009.

Grace III JM, Skaggs RW, Malcom HR, Chescheir GM, Cassel DK. (2003) Influence of thinning operations on the hydrology of a Drained Coastal Plantation Watershed. The Society of Engineering in Agricultural, Food, and Biological Systems, 032038. An ASAE Meeting Presentation.

Grace III JM, Skaggs RM, Cassel DK. (2006) Soil physical changes associated with forest harvesting operations on an organic soil. Soil Science Society of America Journal, 70, 503–509.

Hack JT. (1965) Geomorphology of the Shenandoah Valley Virginia and West Virginia and origin of the residual ore deposits. U.S. Geological Survey Professional Paper 504B. Washington, D.C., pp. B1-B40.

Hack JT, Goodlett JC. (1960) Geomorphology and forest ecology of a mountain region in the central Appalachians. U.S. Geological Survey Professional Paper 347, Reston, Virginia, 66 pp.

Haga H, Matsumoto Y, Matsutani J, Fujita M, Nishida K, Sakamoto Y. (2005) Flow paths, rainfall properties, and antecedent soil moisture controlling lags to peak discharge in a granitic unchanneled catchment. Water Resources Research, 41, W12410.

Harr RD. (1977) Water flux in soil and subsoil on a steep forested slope. Journal of Hydrology, 33(1), 37-58.

Hornbeck JW, Adams MB, Corbett ES, Verry ES, Lynch JA. (1993) Long-term impacts of forest treatments on water yield: a summary for northeastern USA. Journal of Hydrology,150, 323-344, https://doi.org/10.1016/0022-1694(93)90115-P.

Iman RL, Conover WJ. (1983) A modern approach to statistics. New York: John Wiley & Sons.

Japan Forestry Agency. Forest White Paper. Japan Forestry Agency: Tokyo, 2007; pp. 165 (in Japanese).

Jencso KG, McGlynn BL. (2011) Hierarchical controls on runoff generation: Topographically driven hydrologic connectivity, geology, and vegetation. Water Resources Research, 47, W11527.

Jencso KG, McGlynn BL, Gooseff MN, Wondzell SM, Bencala KE, Marshall LA. (2009) Hydrologic connectivity between landscapes and streams: Transferring reach- and plot-scale understanding to the catchment scale. Water Resources Research, 45, W04428.

Jost G, Schume H, Hager H, Markart G, Kohl B. (2012) A hillslope scale comparison of tree species influence on soil moisture dynamics and runoff processes during intense rainfall. Journal of Hydrology, 420-421, 112-124.

Kasahara T, Wondzell SM. (2003) Geomorphic controls on hyporheic exchange flow in mountain streams. Water Resources Research, 39, SBH 3-1-SBH 3-14.

Kiffney PM, Richardson JS, Feller MC. (2000) Fluvial and epilithic organic matter dynamics in headwater streams of southwestern British Columbia, Canada. Archive für Hydrobiologie, 148: 109–129.

Kirkby MJ. (Ed.) (2004) Geomorphology: Critical Concepts in Geography, Volume II, Hillslope Geomorphology, Routledge, London, pp. 16.

Lesch W, Scott DF. (1997) The response in water yield to the thinning of Pinus radiata, Pinus patula and Eucalyptus grandis plantations. Forest Ecology and Management, 99, 295-307, https://doi.org/10.1016/S0378-1127(97)00045-5.

Lim KJ, Park YS, Kim J, Shin Y-C, Kim NW, Kim SJ, Jeon J-H, Engel BA. (2010) Development of genetic algorithm-based optimization module in WHAT system for hydrograph analysis and model application. Computer & Geoscience, 36, 936-944, http://doi.org/10.1016/j.cageo.2010.01.004.

Liu Z, Yao Z, Huang H, Wu S, Liu G. (2012) Land use and climate changes and their impacts on runoff in the Yarlung Zangbo river basin, China. Land Degradation & Development, 1-13, DOI: 10.1002/Idr.1159.

McDonnell JJ. (1990) A rationale for old water discharge through macropores in a steep, humid catchment. Water Resources Research, 26(11), 2821-2832.

McDonnell JJ. (2003) Where does water go when it rains? Moving beyond the variable source area concept of rainfall-runoff response. Hydrological Processes, 17, 1869–1875.

McGlynn B, McDonnell J, Stewart M, Seibert J. (2003) On the relationships between catchment scale and streamwater mean residence time. Hydrological Processes, 17, 175-181.

McGlynn BL, McDonnell JJ, Seibert J, Kendall C. (2004) Scale effects on headwater catchment runoff timing, flow sources, and groundwater-streamflow relations. Water Resource Research, 40, W07504, http://doi.org/10.1029/2003WR002494.

McGuire KJ, McDonnell JJ, Weiler M, Kendall C, McGlynn BL, Welker JM, Seibert J. (2005) The role of topography on catchment-scale water residence time, Water Resource Research, 41,W05002, doi:10.1029/2004WR003657.

McGuire KJ, McDonnell JJ. (2010) Hydrological connectivity of hillslopes and streams: characteristic timescales and nonlinearities. Water Resource Research, 46, W10543.

McNamara JP, Kane DL, Hinzman LD. (1998) An analysis of streamflow hydrology in the Kuparuk River Basin, Arctic Alaska: a nested watershed approach. Journal of Hydrology, 206, 39-57.

Miura S, Hirai K, Yamada T. (2002) Transport rates of surface materials on steep forested slopes induced by raindrop splash erosion. Journal of Forest Research, 7(4), 201-211.

Montgomery DR. (1999) Process domain and river continuum. Journal of the American Water Resources Association, 35: 397–410.

Moore GW, Jones JA, Bond BJ. (2011) How soil moisture mediates the influence of transpiration on streamflow at hourly to interannual scales in a forested catchment. Hydrological Processes, 25, 3701-3710.

Morley TR, Reeve AS, Calhoun AJK. (2011) The Role of Headwater Wetlands in Altering Streamflow and Chemistry in a Maine, USA, Catchment. Journal of American Water Resources Association, 47, 337-349.

Mosley MP. (1979) Streamflow generation in a forested watershed, Water Resource Research, 15, 795–806.

Nanko K, Mizugaki S, Onda Y. (2008) Estimation of soil splash detachment rates on the forest floor of an unmanaged Japanese cypress plantation based on field measurements of throughfall drop sizes and velocities. Catena, 3(72), 348-361, https://doi.org/10.1016/j.catena.2007.07.002.

National Astronomical Observatory. Chronological Environmental Tables MMIX/2010. Maruzen: Tokyo, 2009; pp, 98 (in Japanese).

O'Loughlin EM. (1986) Prediction of surface saturation zones in natural catchments by topographic analysis. Water Resource Research, 22: 794-804.

Onda Y. Current status of discharge and sediment runoff in abandoned plantation forests. Iwanami Shoten: 2010 (in Japanese).

Onda Y, Komatsu Y, Tsujimura M, Fujihara J-i. (2001) The role of subsurface runoff through bedrock on storm flow generation. Hydrological Processes, 15, 1693-1706.

Onda Y, Tsujimura M, Fujihara J-i., Ito J. (2006) Runoff generation mechanisms in high-relief mountainous watersheds with different underlying geology. Journal of Hydrology, 331, 659-673.

Payn RA, Gooseff MN, McGlynn BL, Bencala KE, Wondzell SM. (2009) Channel water balance and exchange with subsurface flow along a mountain headwater stream in Montana, United States. Water Resources Research, 45, W11427.

Payn RA, Gooseff MN, McGlynn BL, Bencala KE, Wondzell SM. (2012) Exploring changes in the spatial distribution of stream baseflow generation during a seasonal recession. Water Resources Research, 48, W04519.

Penna D, Borga M, Sangati M, Gobbi A. (2010) Dynamics of soil moisture, subsurface flow and runoff in a small alpine basin. IAHS Publications, Red Book Series 336, 96–102.

Penna D, Tromp-van Meerveld HJ, Gobbi A, Borga M, Dalla Fontana G. (2011) The influence of soil moisture on threshold runoff generation processes in an alpine headwater catchment. Hydrology and Earth System Sciences, 15, 689-702.

Penna D, Van Meerveld HJ, Oliviero O, Zuecco G, Assendelft RS, Dalla Fontana G, Borga M. (2015) Seasonal changes in runoff generation in a small forested mountain catchment. Hydrological Processes, 29(8), 2027-2042.

Ragan RM. (1968) An experimental investigation of partial area contributions. International Association of Scientific Hydrology Publication, 76, 241-251.

Rahman AA, Hiura H, Shino K, Takese K. (2005)Effects of forest thinning on direct runoff and peak runoff properties in a small mountainous watershed in Kochi Prefecture, Japan. Pakistan Journal of Biological Sciences, 8, 259–266, https://doi.org/10.3923/pjbs.2005.259.266.

Richardson M, Ketcheson S, Whittington P, Price J. (2012) The influences of catchment geomorphology and scale on runoff generation in a northern peatland complex. Hydrological Processes, 26, 1805-1817.

Ruprecht JK, Schofield NJ, Crombie DS, Vertessy RA, Stoneman GL. (1991) Early hydrological response to intense forest thinning in southwestern Australia. Journal of Hydrology, 127, 261-277.

Seibert J, Bishop K, Rodhe A, McDonnell JJ. (2003) Groundwater dynamics along a hillslope: a test of the steady state hypothesis. Water Resource Research, 39(1), 1014.

Sendek KH. (1985) Effects of timber harvesting on the lag time of Caspar Creek watershed. M.S. thesis, Humboldt State University, California, 1985.

Shiklomanov AI, Lammers RB, Vorosmarty CJ. (2002) Widespread decline in hydrological monitoring threatens Pan-Arctic Research. Eos Transactions American Geophysical Union, 83(2): 13–17. DOI:10.1029/2002EO000007.

Sidle RC, Tsuboyama Y, Noguchi S, Hosoda I, Fujieda M, Toshio S. (2000) Stormflow generation in steep forested headwaters a linked hydrogeomorphic paradigm. Hydrological Processes, 14, 369-385.

Sidle RC, Hirano T, Gomi T, Terajima T. (2007) Hortonian overland flow from Japanese forest plantations—an aberration, the real thing, or something in between? Hydrological Processes, 21, 3237–3247, http://dx.doi.org/10.1002/hyp.6876.

Sidle RC, Kim K, Tsuboyama Y, Hosoda I. (2011) Development and application of a simple hydrogeomorphic model for headwater catchments. Water Resource Research, 47, W00H13.

Stednick JD. (1996) Monitoring the effects of timber harvest on annual water yield. Journal of Hydrology, 176, 79-95, https://doi.org/10.1016/0022-1694(95)02780-7.

Strahler AN. (1957) Quantitative Analysis of Watershed Geomorphology. Transaction of the American Geophysical Union, 38: 913-920.

Sugawara M. (1961) On the analysis of runoff structure about several Japanese rivers. Japanese Journal of Geophysics, 2(4), 1–76.

Sun H, Kasahara T, Otsuki K, Saito T, Onda Y. (2016) Spatio-temporal streamflow generation in a small, steep headwater catchment in western Japan. Hydrological Sciences Journal, 1-12, http://dx.doi.org/10.1080/02626667.2016.1266635.

Tateishi M, Xiang Y, Saito T, Otsuki K, Kasahara T. (2015) Changes in canopy transpiration of Japanese cypress and Japanese cedar plantations because of selective thinning. Hydrological Processes, 29(24), 5088-5097, https://doi.org/10.1002/hyp.10700.

Tetzlaff D, Seibert J, McGuire KJ, Laudon H, Burn DA, Dunn SM, Soulsby C. (2009) How does landscape structure influence catchment transit time across different geomorphic provinces? Hydrological Processes, 23, 945-953.

Tromp-Van-Meerveld HJ, Mcdonnell JJ. (2006) Threshold relations in subsurface stormflow 1. A storm analysis of the Panola hillslope, Water Resource Research, 42, W02410, doi:10.1029/2004WR003778.

Tsuboyama Y, Sidle RC, Noguchi S, Hosoda I. (1994) Flow and solute transport through the soil matrix and macropores of a hillslope segment, Water Resource Research, 30, 879– 890.

Turton DJ, Haan CT, Miller EL. (1992) Subsurface flow response of a small forested catchment in the Ouachita mountains, Hydrological Processes, 6, 11 –125, 1992.

Uchida T, Asano Y, Ohte N, Mizuyama T. (2003) Seepage area and rate of bedrock groundwater discharge at a granitic unchanneled hillslope. Water Resources Research, 39, SBH 9-1-SBH 9-12.

Uchida T, Asano Y, Onda Y, Miyata S. (2005) Are headwaters just the sum of hillslopes? Hydrological Processes, 19(16), 3251-3261.

Wagener T, Sivapalan M, Troch PA, McGlynn BL, Harman CJ, Gupta HV, Kumar P, Rao PSC, Basu NB, Wilson J. (2010) The future of hydrology: An evolving science

for a changing world. Water Resource Research, 46, W05301. DOI:10.1029/2009WR008906.

Wainwright J, Parsons AJ, Abrahams AD (2000) Plot-scale studies of vegetation, overland flow and erosion interactions: case studies from Arizona and New Mexico. Hydrological Processes, 14, 2921–2943.

Warburton J. (2010) Sediment transfer in steep upland catchments (northern England, UK): landform and sediment source coupling. landform - structure, evolution, process control, Proceedings of the International Symposium on Landform organised by the Research Training Group 437; Otto J.-C., Dikau R; Springer Berlin Heidelberg: Berlin, Heidelberg: 165-183, http://doi.org/10.1007/978-3-540-75761-0_11.

Ward RC and Robinson M. Principles of hydrology, 450, McGraw-Hill, London: 2010.

Weiler M. (2001) Mechanisms controlling macropore flow during infiltration—dye tracer experiments and simulations. Diss. ETHZ No. 14237.

Weiler M, and Naef F. (2003) An experimental tracer study of the role of macropores in infiltration in grassland soils. Hydrological Processes, 17, 477–493.

Weiler M, and McDonnell JJ. (2007) Conceptualizing lateral preferential flow and flow networks and simulating the effects on gauged and ungauged hillslopes, Water Resources Research, 43, W03403.

Western AW, Blöschl G, Grayson RB. (2001) Towards capturing hydrologically significant connectivity in spatial patterns. Water Resources Research, 37 (1), 83–97.

Whipkey RZ. (1965) Subsurface stormflow from forested slopes, Bulletin - International Association of Scientific Hydrology, 10, 74–85.

Whiting PJ, Bradley JB. (1993) A process-based classification system for headwater streams. Earth Surface Processes and Landforms, 18: 603–612.

Wilks D. Statistical methods in the atmospheric sciences, Volume 100, 3rd ed; Academic Press: 2011.

Wondzell SM, LaNier J, Haggerty R, Woodsmith RD, Edwards RT. (2009) Changes in hyporheic exchange flow following experimental wood removal in a small, low-gradient stream. Water Resources Research, 45, W05406.

Wright KA, Sendek KH, Rice RM, Thomas RB. (1990) Logging effects on streamflow: Storm runoff at Caspar Creek in northwestern California. Water Resource Research, 26(7), 1657-1667, http://do.doi.org/10.1029/WR026i007p01657.

Xiao Q, McPherson EG, Ustin SL, Grismer ME, Simpson JR. (2000) Winter rainfall interception by two mature open-grown trees in Davis, California. Hydrological Processes, 14, 763-784, http://doi.org/10.1002/(SICI)1099-1085(200003)14:4<763::AID-HYP971>3.0.CO;2-7.

Yamazaki Y, Kubota J, Ohata T, Vuglinsky V, Mizuyama T. (2006) Seasonal changes in runoff characteristics on a permafrost watershed in the southern mountainous region of eastern Siberia. Hydrological Processes, 20, 453-467.

Yanai RD; Twery MJ, Stout SL. (1998) Woody understory response to changes in overstory density: thinning in Allegheny hardwoods. Forest Ecology and Management, 102, 45–60.

Zehe E, Sivapalan M. (2009) Threshold behaviour in hydrological systems as (human) geo-ecosystems: manifestations, controls, implications, Hydrology and Earth System Sciences, 13, 1273–1297, doi:10.5194/hess-13-1273-2009, 2009.

Ziemer R.R. (1981) Storm flow response to road building and partial cutting in small streams of northern California. Water Resource Research, 17, http://doi.org/907-917. 10.1029/WR017i004p00907.

Zillgens B, Merz B, Kirnbauer R, Tilch N. (2007) Analysis of the runoff response of an alpine catchment at different scales, Hydrology and Earth System Sciences, 11(4), 1441–1454.